Palaeogeography, Palaeoclimatology, Palaeoecology 683 (2026) 113495

Contents lists available at ScienceDirect

Palaeogeography, Palaeoclimatology, Palaeoecology

journal homepage: www.elsevier.com/locate/palaeo

Metacommunity structural changes of Antarctic benthic invertebrates over the late Maastrichtian

Tasnuva Ming Khan [a,b,c,1,*], Rowan J. Whittle [b], James D. Witts [d], Huw J. Griffiths [b], Andrea Manica [a], Emily G. Mitchell [a,c]

[a] Department of Zoology, University of Cambridge, United Kingdom
[b] British Antarctic Survey, United Kingdom
[c] University Museum of Zoology, Cambridge, United Kingdom
[d] Natural History Museum, London, United Kingdom

ARTICLE INFO

Editor: L Angiolini

Keywords:
Maastrichtian
Ecological complexity
Co-occur
Metacommunities
Antarctica
Extinction patterns
Molluscs

ABSTRACT

Seymour (Marambio) Island, Antarctica has one of the most expanded onshore Cretaceous–Paleogene sedimentary successions in the world. The deposition of the López de Bertodano Formation (~70–65.6 Ma) covered a time of fluctuating sea temperatures, including cold snaps, and warming linked to Deccan Traps volcanism. Here, we study community dynamics of uppermost Cretaceous (Maastrichtian) Antarctic invertebrates using fossils from the Zinsmeister Collection, Paleontological Research Institution, USA, in order to assess ecological complexity prior to the Cretaceous–Paleogene (K–Pg) mass extinction. Our data set consists of 7400 fossils from 85 genera across bivalves, gastropods, cephalopods, echinoderms, brachiopods, scaphopods, polychaetes and octocorals, from 324 localities within six informal sub-units, KLBs 5–9. Due to positional uncertainty of the KLB boundaries, we performed sensitivity analyses to ensure robust results. We found that the number of significantly non-random taxonomic co-occurrences and complexity increased throughout this period. To investigate metacommunity structure that may arise from taxa interactions or environmental filtering, we used the Elements of Metacommunity Structure framework, where we found that taxa replacement, rather than nestedness, increased through time, also highlighting complexity. However, our sensitivity analyses found that our metacommunity results could not be distinguished from sampling biases in the most conservative sensitivity test. Thus, whilst we can be confident that ecological complexity increased throughout the Maastrichtian, the detailed community mechanisms behind this increase cannot be firmly established; nonetheless, this result reinforces the presence of a single, rather than two-fold, K–Pg extinction in the southern high latitudes.

1. Introduction

Mass extinctions have profoundly influenced the history of life, where entire branches have been trimmed from the tree of life (Green et al., 2011). Preferential loss of certain clades, morphologies, trophic levels and functional types reduce the number of possible life history strategies in the immediate aftermath of mass extinctions (Hull, 2015), which can enable entirely new ecological strategies and interactions to evolve (Solé et al., 2002, 2010; Odling-Smee et al., 2013). In the case of the Cretaceous–Paleogene (K–Pg) mass extinction approximately 66 Ma (Bambach, 2006), some major ecological changes included the total extinction of all non-avian dinosaurs on land (Brusatte et al., 2015a), in the oceans, huge losses to planktonic foraminifera and other calcareous plankton (Bown, 2005; Gallala et al., 2009), and the final extinction of ammonoid cephalopod molluscs (Flannery-Sutherland et al., 2024). While marine bivalve molluscs suffered huge taxonomic losses (e.g., rudist bivalves disappeared entirely (Steuber et al., 2002)), functional diversity loss in benthic faunas was minimal (Edie et al., 2018, 2025). In the aftermath of this mass extinction, marine molluscs show increased mobility, predation, and infaunal life habits (Aberhan and Kiessling, 2015), while on land, terrestrial birds exhibited a major radiation (Brusatte et al., 2015b; Field et al., 2018), as did therian and placental

* Corresponding author at: Department of Zoology, University of Cambridge, United Kingdom.
E-mail addresses: tfmk2@cam.ac.uk, tfmkhan27@gmail.com (T.M. Khan).
[1] present address: Department of Geography and Geosciences, GeoZentrum Nordbayern, Friedrich-Alexander-Universität Erlangen-Nürnberg (FAU), Erlangen, Germany

https://doi.org/10.1016/j.palaeo.2025.113495
Received 14 January 2025; Received in revised form 4 December 2025; Accepted 8 December 2025
Available online 9 December 2025
0031-0182/© 2025 The Authors. Published by Elsevier B.V. This is an open access article under the CC BY license (http://creativecommons.org/licenses/by/4.0/).

mammals (O'Leary et al., 2013; Grossnickle and Newham, 2016). In the high latitudes, where the marine mass extinction was equally as severe in terms of taxonomic losses in key groups as in the lower latitudes (Witts et al., 2016), most work has focused on the extinction horizon itself (Witts et al., 2015, 2016), and the subsequent biotic recovery (Crame et al., 2014; Whittle et al., 2019). To date, no quantitative work has focused on the pre-extinction Maastrichtian Stage, an understanding of which is necessary to truly contextualize the scale of the K–Pg transition.

Studying broad, pre-extinction ecological dynamics requires consistent stratigraphy with no significant depositional hiatuses, minimal time averaging, and a well sampled fossil record. Seymour (Marambio) Island is perfect for such ecological studies because it fulfils all of the criteria above. It contains a continuous sequence (no major hiatuses) of almost 40 million years including an expanded record of the K–Pg mass-extinction interval (Crame, 2019; Reguero, 2019). At ~65°S palaeolatitude, it is the highest latitude onshore locality for this time period in either hemisphere (Crame, 2019), allowing for the study of environmental and biological processes in the polar regions. The island is located in the James Ross Basin of the Antarctic Peninsula (Fig. 1), with highly expanded rock exposures of Maastrichtian (Late Cretaceous, approximately 71 Ma) to Late Eocene (approximately 33 Ma) age (Rinaldi, 1992; Hathway, 2000; McArthur et al., 2000; Francis et al., 2006; Olivero, 2012). This record means that it is a key locality for investigating palaeoclimate, palaeoenvironments and biotic evolution (Anderson et al., 2011; Olivero, 2012; Douglas et al., 2014; Barreda et al., 2015) over a time period of almost 40 million years. Palaeobiological and evolutionary insights from Seymour Island include the development of cool temperate Palaeogene climates within the Weddellian Biotic Province (Case, 1988) which were dominated by *Nothofagus* forests (Askin, 1988), the preferential dispersal of small marsupial mammals over placental mammals between South America and Australia (Case et al., 1988), the asynchronous effects of the Marine Mesozoic Revolution (Whittle et al., 2018), periodic returns of the benthic community to Palaeozoic-like community structure with low predation in the Eocene (Aronson et al., 1997), the origins of Southern Ocean benthic fauna (Aronson and Blake, 2001; Crame et al., 2014), the evolution of penguins (Jadwiszczak, 2006) and apex predation on the Antarctic continent (Acosta Hospitaleche and Jones, 2024).

The nature of the K–Pg extinction in Antarctica has been debated, with hypotheses suggesting it was either gradual (Zinsmeister et al., 1989; Zinsmeister, 1998), multi-phased (Tobin et al., 2012; Tobin, 2017) or a single event (Springer, 1990; Marshall, 1995; Witts et al., 2015, 2016). The gradual extinction hypothesis was attributed to macrofossil first and last occurrence data from an "expanded" K–Pg interval, prior to the precise placement of the K–Pg boundary in the Antarctic sequence. During this expanded interval, spanning approximately 50 m of stratigraphy, last occurrences continually increased, while first appearance dates of taxa remained continuous throughout the Maastrichtian (Zinsmeister et al., 1989). Zinsmeister argued that a single catastrophic extinction should show a cluster of last appearances, which would be followed by a cluster of first appearances (Zinsmeister et al., 1989). Under the multi-phased extinction hypothesis, confidence intervals placed on last appearance datums derived from existing fossil range data from older publications and individual sedimentary section lines, identified two distinct clusters of last appearances, one at the (now defined) K–Pg boundary affecting nektonic molluscs, and a precursor extinction approximately 40 m below the boundary, primarily affecting the benthic component (Tobin et al., 2012; Tobin, 2017). This precursor extinction was linked with oxygen isotope evidence for climate warming, linked temporally to the Late Maastrichtian Warming Event and Deccan Trap volcanism (Tobin et al., 2012; Barnet et al., 2018; Hull et al., 2020). Early assessments of the extinction pattern based solely on the fossil record of ammonites however, suggested that their extinction pattern was most likely sudden, rather than gradual (Springer, 1990; Marshall, 1995). The single, catastrophic extinction hypothesis used

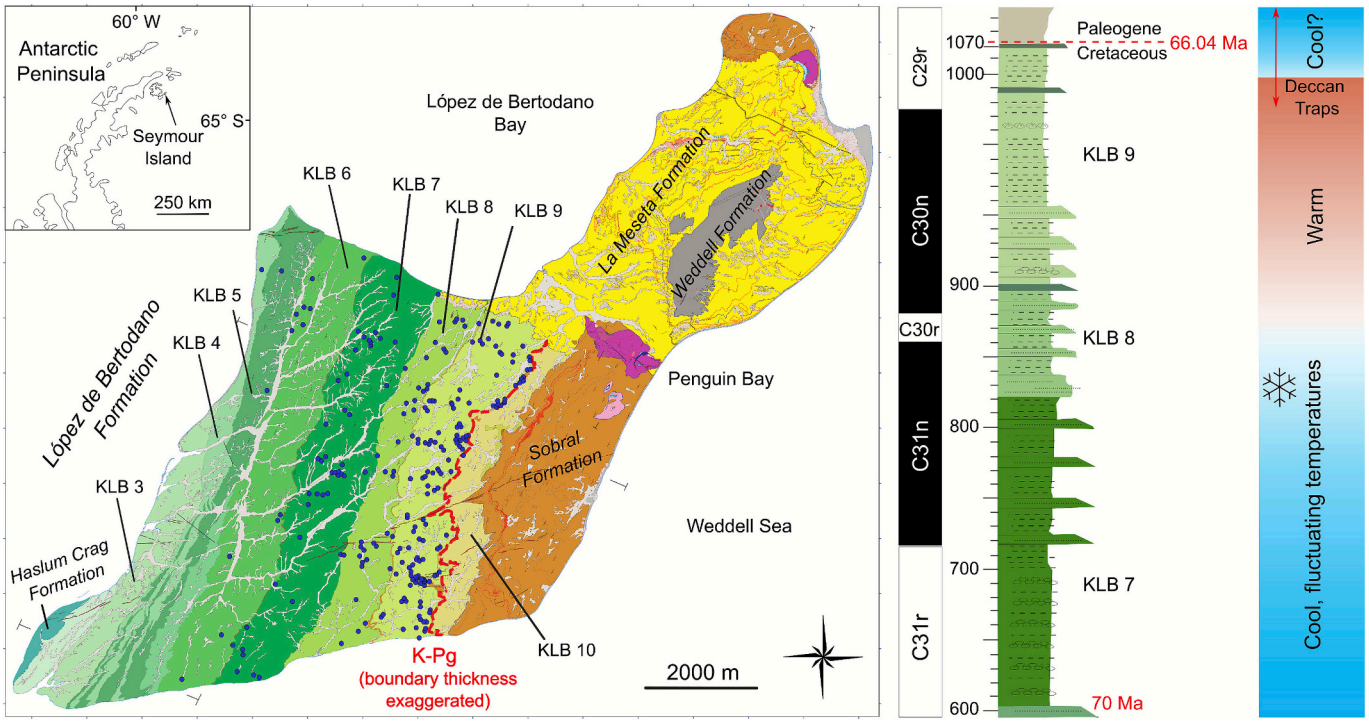

Fig. 1. Simplified geological map of Seymour (Marambio) Island, with the López de Bertodano Formation expanded into the informal cartographic mapping units KLBs 2–10, modified from Crame et al. (2014); Montes et al. (2019b). Composite stratigraphy of the Molluscan Allomembers (KLBs 7–9), along with magnetostratigraphic dates, modified from Montes et al. (2019b). Palaeoclimatic interpretation is derived from Bowman et al. (2013) and Witts et al. (2016), rescaled to fit the stratigraphic log, using the K–Pg boundary and glauconite-rich beds as tie-points. Blue dots on the map show sampling localities in this study. (For interpretation of the references to colour in this figure legend, the reader is referred to the web version of this article.)

newer composite range data from multiple British Antarctic Survey measured sections. Based on internally consistent and updated taxonomic identifications, these studies identified a 61 % species level and 36 % generic level loss in benthic molluscs and loss of all nektonic ammonites at the K–Pg boundary itself, after modelling range extensions to counter for the Signor-Lipps effect (Witts et al., 2016; Whittle et al., 2019). Further difficulties between drawing exclusive causal links between Deccan Traps-induced warming are because proxy evidence for general climate warming commenced 2 million years prior to the hypothesized precursor extinction in Antarctica, resulting in a mismatch in timing (Bowman et al., 2013; Witts et al., 2016).

Beyond the use of presence/absence data, the spatio-temporal ecological complexity of Cretaceous communities on Seymour Island has the potential to shed some light on the nature of the end-Cretaceous mass extinction in Antarctica, as complexity correlates to ecosystem resilience (Pimm, 1984), with extinction patterns determining expected changes in ecological complexity. Measures of complexity include species richness, connectance and the frequency of interactions (Proulx et al., 2005). Here, we define "complexity" to mean structured co-occurrences of taxa, i.e., a measure of how often species significantly aggregate or segregate across the different sites through space and time, and we assess complexity at taxa level and at the metacommunity level. We expect complexity to increase up-section till the K–Pg boundary under a catastrophic extinction scenario, and complexity to decrease up-section prior to the K–Pg boundary under a gradual extinction scenario.

1.1. The elements of metacommunity structure

We assess complexity as significantly non-random pairwise relationships between taxa and at the metacommunity level, employing a method known as Elements of Metacommunity Structure, currently best studied in lake ecosystems (Cottenie and De Meester, 2003; Heino, 2005; Allen et al., 2011; Logue et al., 2011; Podani and Schmera, 2011; Heino et al., 2015a, 2015b, 2015c; Datry et al., 2016), but which has also recently been applied to the fossil record (García-Girón et al., 2021; Eden et al., 2022). In this study we define metacommunity as a set of local communities that are potentially connected to each other by dispersal, while a community is a group of species within a given site (Leibold and Mikkelson, 2002). Community structure is the patterning of co-occurrences across different sites, and may be driven by species sorting (due to environmental differences), mass effects (due to high dispersal pressure), patch dynamics (due to competition or colonization), or neutral effects (due to random dispersal and stochastic events) (Leibold et al., 2004; Leibold and Mikkelson, 2002; Presley et al., 2010). The Elements of Metacommunity Structure (EMS) framework provides a toolkit to identify distribution patterns and infer these underlying organizational processes using a pattern-based approach, where characteristics of an ordinated, site-by-taxa community composition matrix, can reveal spatial patterns along inferred environmental gradients (Leibold and Mikkelson, 2002; Presley et al., 2010; Dallas, 2014). Reciprocal averaging is the best indirect ordination procedure to discern sample variation in response to environmental gradients (Gauch et al., 1977; Pielou, 1984). Three hierarchical properties are assessed in the EMS framework: coherence, turnover, and boundary clumping (Leibold and Mikkelson, 2002; Presley et al., 2010).

Coherence measures the degree to which a distributional pattern can be collapsed into a single ordination axis, i.e., whether species' distributions respond to a common environmental gradient (Leibold and Mikkelson, 2002). It does so by measuring the correlation between embedded absences in ordinated incidence matrices (i.e., whether certain species tend to avoid each other or preferentially occur together), and then comparing the observed value to a null distribution of embedded absences from 1000 simulated matrices (Leibold and Mikkelson, 2002; Presley et al., 2010; Dallas, 2014). When embedded absences are not significantly different from the null model, the structure is described as "random", in that taxa are distributed at random with respect to the axis of ordination, which suggests that taxa are not responding to a common environmental gradient (Leibold and Mikkelson, 2002; Presley et al., 2010). When embedded absences are significantly larger than expected by chance, coherence is negative, and a "checkerboard" pattern emerges, which indicates high numbers of mutually exclusive taxa. The ecological interpretation behind a checkerboard pattern is that of niche segregation and/or competitive exclusion between taxa (Diamond, 1975; Leibold and Mikkelson, 2002; Presley et al., 2010). When embedded absences are significantly lower than the null distribution, coherence is significantly positive, which indicates that species' distributions are responding similarly to a common environmental gradient, the inference being that this common response is due to similarities in evolutionary history or ecological preferences (Leibold and Mikkelson, 2002; Presley et al., 2010).

For communities that have positive coherence, the second EMS metric to be evaluated is turnover. Turnover occurs where the spatial ranges of two species mismatch, and measures the amount of spatial replacement of species between sites along an ordination axis (i.e, environmental gradients) (Leibold and Mikkelson, 2002; Presley et al., 2010). It is calculated by comparing replacements against a null distribution, where the entire spatial range of each taxon is shifted at random (Dallas, 2014; Leibold and Mikkelson, 2002; Presley et al., 2010). Prior to this calculation, the taxon ranges are made artificially coherent by filling in any embedded absences, as absences within the gradient are stochastic (Presley et al., 2010). When turnover is significantly negative (i.e., species are replaced less often than expected by chance), the species ranges along the environmental gradient are "nested", meaning that species-poor sites contain subsets of those found at species rich sites (Supplementary Fig. S1). This nested pattern infers species loss without replacement (Leibold and Mikkelson, 2002; Presley et al., 2010), for example due to habitat degradation, or along island biogeography systems where smaller islands hold subsets of larger islands. When turnover is significantly positive (i.e., species are actively being replaced along the gradient), the species' ranges along the gradient are "non-nested", forming distinct communities over this gradient (Leibold and Mikkelson, 2002; Presley et al., 2010). The spatial turnover metric is depicted in Supplementary Fig. S1. When the turnover observed does not differ significantly from the null distribution, the organizational processes are considered to be weaker, therefore the structures are described as "quasi"-structures.

The final parameter, boundary clumping, is used to assess where on the environmental gradient the species' range limits lie (i.e. how often multiple taxa have their range limits in the same study sites), and is calculated using Morisita's Index, MI (Morisita, 1962). When multiple species' ranges end at the same position, the boundary is described "clumped" ($MI > 1$), whereas if the range ends are more evenly distributed, the boundary is "evenly spaced" ($MI < 1$). When the range boundaries are random and $MI \approx 1$, the boundary is described as "random".

The combination of these properties forms one of 14 idealized metacommunity structures, which are defined in Table 1 and two end-members of these metacommunities are depicted in Supplementary Fig. S1.

In order to understand how the underlying metacommunity structure relates to different taxa, we analysed the frequency of pairwise associations between taxa using a combinatorics approach to see the extent to which pairwise co-occurrences occur significantly more or less than random (Veech, 2013). Significantly non-random co-occurrences indicate shared ecological or evolutionary processes between the taxa pair (Blanchet et al., 2020), i.e. not necessarily direct taxa interactions, but also environmental (dis)associations (Blanchet et al., 2020).

1.2. Geological setting

Six geological units are present on Seymour Island; here we focus on the López de Bertodano Formation (LBF) (Maastrichtian, ~71–65.6 Ma)

Table 1
A glossary of the most important terms in this manuscript. Table adapted from (Leibold and Mikkelson, 2002; Presley et al., 2010; Heino et al., 2015a; García-Girón et al., 2021; Eden et al., 2022).

Concept	Description and ecological interpretation
Community	A group of taxa at a particular site (Leibold and Mikkelson, 2002).
Metacommunity	A set of local communities that are potentially connected to each other by dispersal (Leibold and Mikkelson, 2002).
Complexity	Structured co-occurrences of taxa, i.e., a measure of how often taxa preferentially aggregate or segregate, at the community and the metacommunity level.
Elements of metacommunity structure	A toolkit proposed by Leibold and Mikkelson (2002) and expanded by Presley et al. (2010) to infer metacommunity properties from ordinated site-by-taxon incidence matrices, in order to infer biological processes from spatial patterns. Can be assessed using the "metacom" package (Dallas, 2014).
Reciprocal ordination	Ordering an incidence matrix so sites with the most similar taxa are grouped together and taxa with the most similar distributions are grouped together (Leibold and Mikkelson, 2002)
Environmental gradient	The first axis of the ordination, which reveals a latent gradient that structures the spatial distribution of taxa (Leibold and Mikkelson, 2002; Presley et al., 2010).
Coherence	A measure to which degree taxa distributions respond to a common environmental gradient (a single axis). Positive coherence indicates taxa respond to the same gradient and negative coherence indicates that taxa do not share this response.
Range turnover	The amount of spatial replacement of taxa between sites along an ordination axis. Negative values indicate taxa loss and positive values indicate taxa replacement.
Range boundary clumping	The degree to which taxa's end limits cluster at the same sites.
Random structure	No metacommunity structure is detected when coherence does not vary significantly from the null expectation.
Checkerboard structure	Negative coherence, indicate high numbers of mutually exclusive pairs due to strong segregation.
Nested clumped structure	Positive coherence; significant negative turnover; positive boundary clumping. Taxa poor communities are subsets of taxa rich communities, with groups of taxa lost together due to shared range ends on the gradient. When turnover is non-significant, the community is more weakly structured and termed "quasi-nested clumped".
Nested random structure	Positive coherence; significant negative turnover; non-significant boundary clumping. Taxa poor communities are subsets of richer communities with random taxon loss as range boundaries are randomly distributed on the gradient, i.e., weak environmental filtering. When turnover is non-significant, the community is more weakly structured and termed "quasi-nested random".
Nested hyper dispersed structure	Positive coherence, significant negative turnover, negative boundary clumping. Taxa poor communities are subsets, with taxon loss regularly occurring along the gradient. When turnover is non-significant, the community is more weakly structured and termed "quasi-nested hyper dispersed".
Clementsian structure	Positive coherence, significant positive turnover, positive boundary clumping. Taxa are organized into cohesive groups with shared tolerances, with distinct groups replacing each other sharply over the gradient due to strong environmental filtering. Responses are community-level rather than at taxon level. When turnover is non-significant, the community is more weakly structured and termed "quasi-Clementsian".
Gleasonian structure	Positive coherence, significant positive turnover, non-significant boundary clumping. Taxa distributions are individualistic with gradual replacements on the environmental gradient due to niche sorting. When turnover is non-significant, the community is more weakly structured and termed "quasi-Gleasonian".
Evenly spaced structure	Positive coherence, significant positive turnover, negative boundary clumping. Taxa have non-overlapping and regularly spaced niches along the gradient, with regular replacements. When turnover is non-significant, the community is more weakly structured and termed "quasi-evenly spaced".

(Rinaldi et al., 1978). The LBF crops out continuously over approximately 70 km^2 (Crame et al., 2004) on the southwest side of the island, and is unconformably bounded by the Haslum Crag Formation (early Maastrichtian Stage) at the base, and overlain by the Sobral Formation (Danian –?Thanetian; Paleogene) (Pirrie et al., 1991; Olivero et al., 2008). The LBF is 1100 m thick, comprised of relatively homogeneous and unconsolidated clayey-silts and silty-clays, with intercalated thin burrowed sandstone horizons, and layers of early diagenetic carbonate concretions (Macellari, 1988; Bowman et al., 2012). Subdivision of the LBF has been hampered by a high degree of lithological homogeneity at outcrop scale (Macellari, 1988; Bowman et al., 2012). It was originally divided into ten informal cartographic units based on "differences in lithologic, faunal and physiographic characteristics" (Macellari, 1988), and "the contacts were drawn at distinctive beds that are easy to trace laterally on aerial photographs" (Macellari, 1984). Because of their nearly uniform lithology, the mappable units were not considered distinctive enough to warrant Member status (Macellari, 1984, 1988). The units were termed KLBs (an acronym for "Cretaceous López de Bertodano"), with KLB 1 being the oldest, and KLB 10 the youngest (Fig. 1) (Macellari, 1984, 1988). Recognizing these units in the field is, however, challenging due to the aforementioned lithological homogeneity, but the palaeontological content of the LBF allows clustering into two larger informal units: the "Rotularia Units" (KLBs 1–6) and "Molluscan Units" (KLBs 7–10) (Macellari, 1988).

The Cretaceous-Paleogene boundary occurs at the top of KLB 9, near the base of a prominent glauconite-rich bed, termed the "Lower Glauconite" (Elliot et al., 1994; Zinsmeister, 1998), defined as subunit 9g in the most recent geological map (Montes et al., 2019b). A small iridium (Ir) anomaly has been recorded at/just below this level, fallout from the Chicxulub asteroid impact which link the boundary to others around the globe (Elliot et al., 1994; Molina et al., 2006; Ferreira Da Silva et al., 2023). Since the original description of the LBF, the basal unit (KLB 1) has now been assigned to the Haslum Crag Formation (Olivero et al., 2008). Subsequent mapping efforts retained the KLB boundaries (Brecher and Tope, 1988). The most recent geological map of Seymour Island (Montes et al., 2019b) continues to use the KLB subdivisions as mappable units, and further divides the LBF into three members based on lithostratigraphic features and palaeontological content (Montes et al., 2019a): the Rotularias Allomember (lower, comprising of KLBs 2–6); the Molluscan Allomember (middle, comprising of KLBs 7–9); and the Cenozoic Allomember (upper, comprising of KLB 10, but divided into units 10–11 (Montes et al., 2019b)).

Integrated age models for the LBF have been compiled based on strontium isotope chemostratigraphy (McArthur et al., 1998; Crame et al., 2004), ammonite and dinoflagellate cyst biostratigraphy (Bowman et al., 2012, 2013; Witts et al., 2015) and magnetostratigraphy (Tobin et al., 2012). The magnetostratigraphic chrons C31R through C29N on Seymour Island suggest an early Maastrichtian–Danian age for the sequence (Tobin et al., 2012). The most recent chronostratigraphic age models indicate that the base of the Molluscan Allomember (base of KLB 7) is dated to ~70.0 Ma, and the K–Pg boundary (top of KLB 9) at 66.04 Ma (Montes et al., 2019a) (Fig. 1).

The LBF was deposited in a shallow marine (shelf) environment, under variable water depths. The friable texture and lack of diagnostic sedimentary structures make the interpretation of the depositional environment difficult. Palaeoenvironmental interpretations of the basal

LBF have differed, with shallow water, nearshore deposition originally proposed based on mudstone facies and the presence of flaser bedding (Macellari, 1988; Olivero et al., 2007, 2008). An alternative interpretation of deeper water outer shelf conditions was also proposed, due to a slight decrease in grain size up-section from the Haslum Crag Formation (Crame et al., 2004). The middle to upper sections of the LBF represent overall transgression (sea level rise) and mid-outer shelf environments (Macellari, 1988; Olivero, 2012). In the uppermost 300 m of the LBF (the Molluscan Allomember) and across the K–Pg boundary, a regressive phase (sea level fall) has been suggested (Olivero, 2012). The occurrence of glauconite-rich beds, especially at the top of KLB 8 and at the K–Pg boundary, suggest that deposition on the shelf was interrupted by periods of slow, condensed and uniform sedimentation (Elliot et al., 1994; Olivero et al., 2017). Proxy data from palynological, palaeobotanical and marine macrofossil records suggest overall cool and humid conditions (Askin, 1988; Bowman et al., 2012), with terrestrial and marine temperatures ranging between ~4–15 °C, and at least three particularly cold spells during the mid–late Maastrichtian, when sea ice may have formed (Bowman et al., 2013). The last such cold snap is depicted in Fig. 1. This was followed by climate warming that began ~2 million years before, and ended just prior, to the K–Pg boundary (Bowman et al., 2013), with marine temperatures increasing by as much as 7.8 ± 3.3 °C (Petersen et al., 2016).

Here we study benthic taxa from the most macrofossil-rich part of the section, the Molluscan Allomember (KLBs 7–9), to assess metacommunity ecological complexity during the late Maastrichtian. We quantify ecosystem structure in the run up to the K–Pg mass extinction using metacommunity and co-occurrence analyses and contextualize the true impact of this global evolutionary event.

2. Methods

2.1. Data collection

The data used in this study were collected from Seymour Island by Zinsmeister and colleagues, over several field seasons in the 1980s (Zinsmeister, 1982, 1985; Zinsmeister et al., 1989). Fossil molluscs, comprising mostly of bivalves, gastropods, and ammonites, were collected along six stratigraphic sections from around the island in 1982 and 1984 (Macellari, 1984, 1988). Hundreds more macrofossil localities were later sampled along the K–Pg boundary (Zinsmeister et al., 1989), which were projected onto a single vertical section, using a method termed stratigraphic plane analysis (Zinsmeister, 2001). These field campaigns yielded almost 22,000 fossil specimens of Cretaceous to Eocene age, which have, since April 2009, been housed in the William J. Zinsmeister Collection of the Paleontological Research Institution (PRI), Ithaca, NY, USA (Dietl, 2010). Prior to PRI's acquisition of Zinsmeister's specimens, one of the largest collections of Antarctic fossils in the world was inaccessible to researchers outside of Purdue University or Ohio State University (Dietl, 2010). Since PRI's acquisition of Zinsmeister's fossils, PRI Collections staff have digitally catalogued all the material (searchable on www.pricollectionsdatabase.org), photographed many of the specimens, publicly exhibited exceptional specimens at the Museum of the Earth, and created 3D models of numerous taxa as part of a virtual collection enabling the study of this collection.

Using the PRI Collections we collated abundance and updated (where needed) the taxonomic identifications to align with newer publications (Beu, 2009; Crame et al., 2014). The PRI collections retain the genus and species level identifications that were originally assigned to each specimen by Zinsmeister and colleagues. Subsequent work by other authors, including those on more recently collected fossils (Crame et al., 2004; Witts et al., 2016; Whittle et al., 2019) have updated the taxonomic status of many molluscan taxa from Seymour Island (Beu, 2009; Crame et al., 2014). Conflicts between the Zinsmeister and British Antarctic Survey (BAS) nomenclature are detailed in the taxonomic appendix of Crame et al. (2014). We resolved these discrepancies in two ways: (i) we reassessed all uncertain genus names against specimens in the PRI image database, deleted known errors and corrected updated names, and (ii) coarsened our data to assess all ecological associations at the Family level. This left us with a total of 48 benthic families for our analyses.

Fossil specimens in the Cretaceous section of the Zinsmeister Collection are organized by geographic locality (324 "stations" in PRI terminology), the verbatim coordinates for which were derived by PRI Collections staff, using stratigraphic plane analyses, as detailed in Stilwell et al. (2004). PRI Collections staff additionally transcribed all stations from field maps onto Google Earth. In most cases the field marked locality and formula derived locality plotted very close to each other, with the formula derived coordinates plotting generally northwest of the marked localities. Some localities could not be located on field maps and were noted in the Collections database; excluding these uncertain stations left 270 sites for analyses. As the original fossil specimens were collected to assess spatiotemporal patterns along informal cartographic KLB units, we plotted all the coordinates (using PRI's field map-located reported latitude and longitude) onto the most recent geological map of Seymour Island in QGIS (Montes et al., 2019b), and assigned a KLB unit number to each station. To ensure consistency with the PRI Collections, we chose to divide our analyses along KLB subdivisions. Stations that contained all the benthic fauna characteristic of cold methane seeps (*'Lucina' scottii, 'Thyasira' townsendi, Solemya rossiana*, Little et al., 2015) were also excluded from our study. These data filters left us with a total of 259 stations spanning KLBs 5–10, but we focus on KLBs 7–9 (Molluscan Allomember units – uppermost Maastrichtian) only for a total of 204 stations, because KLBs 5, 6 and 10 did not have sufficient localities to enable comparable analyses.

2.2. Sampling completeness

We performed all analyses in R (R Core Team, 2022) (see deposited code; Khan et al. (2025a)). Data from the benthic members of the Molluscan units came from 37 sites in KLB 7, with 29 families present, 30 sites in KLB 8, with 30 families present, and 137 sites in KLB 9, with 42 families present (Table 2). In order to assess whether the majority of taxa present at each KLB have been collected, we analysed accumulation curves at the family level for the Molluscan Allomembers as a whole, and per KLB, using abundance data in the R package vegan (Oksanen et al., 2022). Due to uneven sampling effort per KLB, we also calculated the expected family richness of each KLB unit at 95 % coverage sampling (Chao et al., 2014) using the R package iNEXT (Hsieh et al., 2024). Accumulation and coverage-based curves are presented in Supplementary Fig. S2, and the expected richness values are present in Supplementary Table 1.

2.3. Ecological analysis

For ecological analyses we used binary presence/absence data based on the fossils found in each station (c.f. Klompmaker and Finnegan, 2018; Eden et al., 2022). Occurrence data by station can be found via the UK Polar Data Centre (Khan et al., 2025b).

2.3.1. Ordination

Ordination methods summarize the multivariate nature of community data along a reduced number of axes representing the main trends. We applied two-axis NMDS on Jaccard dissimilarities to explore variation among the sites in KLBs 7, 8 and 9. We also performed reciprocal averaging on the same data to visualize taxonomic similarity and to evaluate whether any temporal structure was evident at the KLB level.

2.3.2. Pairwise co-occurrences

We use the cooccur package (Griffith et al., 2016) in R to assess the percentage of non-random associations between taxa in sites in KLB 7, KLB 8, and KLB 9. Taxa which only occur in one site were removed from

Table 2
Families in each of the Molluscan Allomembers. Families that were found only in one locality (singletons), are highlighted with asterisks.

Unit	Group	Families present
KLB 7	Bivalves	Chamidae*, Corbulidae, Cucullaeidae, Gryphaeidae, Hiatellidae, Lahillidae*, Limidae*, Limopsidae*, Nuculidae, Pholamyidae, Pinnidae, Thraciidae*, Veneridae
	Corals	Flabellidae*
	Gastropods	Amberleyidae, Aporrhaidae, Cassidae, Cerithiidae*, Fasciolariidae, Gordenellidae*, Naticidae*, Perissityidae, Pleurotomariidae, Taiomidae, Vanikoridae
	Lobsters	Nephropidae
	Polychaetes	Serpulidae
	Scaphopods	Dentaliidae
KLB 8	Bivalves	Corbulidae, Cucullaeidae, Entoliidae*, Gryphaeidae, Hiatellidae, Lahillidae, Limidae*, Limopsidae*, Nuculidae, Pinnidae*, Pulvinitidae*, Thraciidae*, Trigoniidae, Veneridae
	Corals	Turbinoliidae*
	Echinoderms	Isselicrinidae*, Cidaridae
	Gastropods	Amberleyidae, Aporrhaidae, Cassidae, Cerithiidae*, Fasciolariidae, Perissityidae, Pleurotomariidae, Taiomidae, Vanikoridae
	Lobsters	Nephropidae
	Polychaetes	Serpulidae
	Scaphopods	Dentaliidae
KLB 9	Bivalves	Corbulidae, Cucullaeidae, Entoliidae, Gryphaeidae, Hiatellidae, Lahillidae, Limidae, Malletiidae, Mytilidae*, Nuculidae, Bakeveliidae, Periplomatidae*, Pholadomyidae, Pinnidae, Pteriidae, Pulvinitidae, Solemyidae*, Thraciidae*, Trigoniidae, unidentified*, Veneridae
	Corals	Flabellidae, Fungiacyathidae
	Echinoderms	Isselicrinidae, Cidaridae*
	Gastropods	Acteonidae*, Amberleyidae, Aporrhaidae, Cassidae, Cerithiidae, Fasciolariidae, Naticidae, Perissityidae, Pleurotomariidae, Taiomidae, Turritellidae, unidentified*, Vanikoridae
	Lobsters	Nephropidae
	Octocorals	Waiparaconidae*
	Polychaetes	Serpulidae
	Scaphopods	Dentaliidae

the analyses because they disproportionally impact the co-occurrence analyses (Collins et al., 2011; Pitta et al., 2012). Exclusion of singletons left 20 families in KLB 7 (nine singletons), 20 families in KLB 8 (ten singletons) and 34 families in KLB 9 (eight singletons) (Table 2). The cooccur framework has a very low rate of Type I and Type II errors, provided that the number of sites assessed is greater than 20 (Veech, 2013), so it is robust to differences in sampling for this number of sites and above.

2.3.3. *Metacommunity analyses*

We analysed binary presence/absence data from the stations in KLBs 7–9. Here, each station is a community while all of the stations within a particular KLB forms a metacommunity. On reciprocally ordinated data, we calculated the observed coherence, turnover and boundary clumping values for each KLB using the R package metacom (Leibold and Mikkelson, 2002; Presley et al., 2010; Dallas, 2014). We used simulations of these parameters to determine whether the observed values differed significantly from simulated mean values, normalizing them as *Z*-scores. These Coherence, Turnover and Boundary Clumping values were used to determine the inferred metacommunity structure of each KLB unit (Dallas, 2014) (Table 1).

2.4. *Sensitivity analysis*

The Zinsmeister Collection, though expansive, has been challenging to use due to uneven sampling effort and absence of data tied directly to detailed measured sections (Crame et al., 2014). In this study, we have chosen to quantify the impact of these challenges so the Collection may be better utilized. This work is particularly important, as museum collections are a crucial resource of historic data that help us understand patterns and processes of past evolutionary and ecological changes, that would otherwise be unavailable (Nicholson, 1991). For example, it has been demonstrated that "hidden" museum collections probably hold as much as 23 times more data than are currently accessible through global compendia such as the Paleobiology Database (PBDB) (Marshall et al., 2018).

There are two potential sampling influences in our data, to which we apply sensitivity analyses to understand their impact on our results. The first deals with locality position uncertainty, and second is variation in sampling intensity.

First, the stratigraphic plane analyses used by Zinsmeister allow for assessment of synchronous spatial patterns (Zinsmeister et al., 1989; Stilwell et al., 2004). However, there are two complications with this method: (i) the subdivision into the cartographic KLB units is challenging in the field due to lithological homogeneity (Bowman et al., 2012), leading to uncertainties in the positional boundaries of the KLBs, and (ii) the projection plane method produced a number of stratigraphic ranges for different taxa that contrast significantly with BAS data tied to measured section lines (Crame et al., 2014).

In order to test how potential uncertainties in locality co-ordinates impacted our results we performed sensitivity analyses as follows: for each KLB unit in our study (KLBs 7, 8 and 9), we applied a set of sensitivity analyses (Fig. 2) to adjust the positional boundaries of the KLB units, and performed ecological analyses both on raw and treated data. The boundary of KLB 9 and 10 (namely the K–Pg) was kept fixed because it is now well defined (e.g., Montes et al., 2019a).

1) For KLBs 7 and 8, we shifted the boundaries to the west by approximately 250 m, which incorporated some stratigraphically older stations, and excluded some younger sections (Fig. 2a).

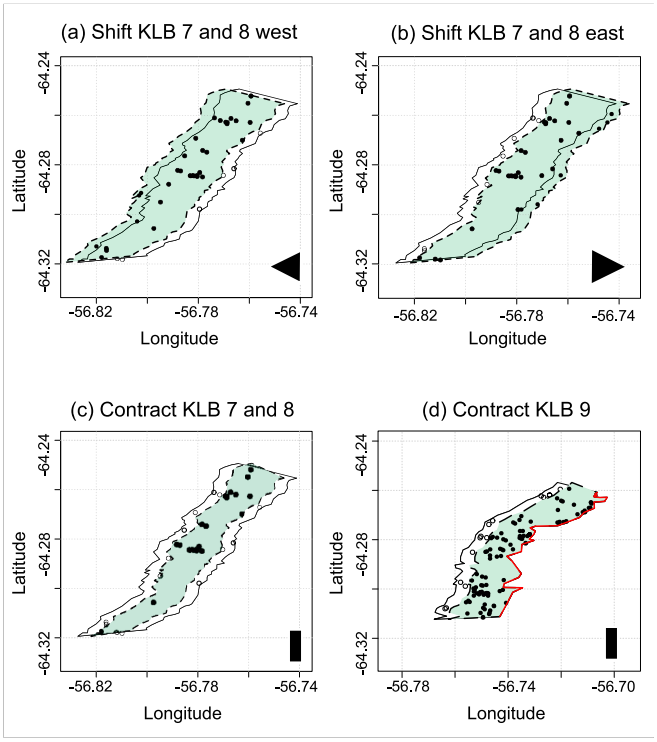

Fig. 2. (a-c) Sensitivity analyses applied to the KLB 7 and 8 units. (d) The K–Pg boundary was held fixed, so KLB 9 could only be contracted in one direction. Black symbols summarize the nature of the sensitivity test; these symbols are used in the results figures, namely shifting west, shifting east, then contracting the boundaries.

2) We also shifted the boundaries of KLB 7 and 8 to the east by approximately 250 m, which incorporated some stratigraphically younger stations, while excluding older stations (Fig. 2b).
3) We contracted any given KLB by 250 m on each side (Fig. 2c). This ensure that only the localities that definitely belonged in the KLB (as opposed to the localities closer to the positional boundaries), were included.
4) For KLB 9 we held the K–Pg boundary fixed, then moved the bottom of KLB 9 boundary west as above. This allowed only for the contraction of KLB 9, instead of also shifting the whole unit east or west (Fig. 2d).

These sensitivity analyses were designed specifically to address the concern of positional boundaries of KLB units due to homogeneous lithology at outcrop scale, and from reconciling field-marked localities with coordinates derived from stratigraphic plane projections. Raw results, as well as treated results, are reported here.

We further minimised the stratigraphic range uncertainty between BAS and Zinsmeister data by using only presence/absence data, assessing our taxonomic co-occurrences at family level (instead of genus or species level), and at a relatively coarse temporal resolution (subdivisions of the Molluscan units) instead of much finer temporal scales, similar to previous palaeontological studies using these methods (e.g. García-Girón et al., 2021; Eden et al., 2022).

We considered dividing KLB 9 into sub-sections in order to further test the hypothesized double extinction some 30–60 m below the K–Pg boundary (Tobin, 2017). However, this was not possible as we would have had to divide our spatial data explicitly according to which stations fall above and beneath the hypothesized first extinction horizon. A reassessment of the measured sections in the earliest data sources (Macellari, 1984, 1988) revealed two problems: (i) only 14 stations fell between the interval starting at 60 m below the K–Pg boundary, a number too few for meaningful metacommunity or pairwise cooccurrence analyses (Veech, 2013), (ii) at the time of Macellari's data collection, the precise location of the K–Pg boundary was not yet fixed (Zinsmeister, 1998), meaning that it is impossible to determine which stations should be included in the first interval. Subsequently collected Zinsmeister data (Zinsmeister et al., 1989), which were plotted by Tobin (2017), are not presented spatially either, making comparisons with our methods untenable. The only way to reassess spatial (therefore, largely contemporaneous) ecosystem complexity in these crucial intervals is to collect new data, with fossils sampled perpendicular to strike on multiple section lines laterally along the length of the K–Pg boundary, with collections made both above and below the hypothesized pulsed extinction interval levels.

Secondly, we tested the impact of sampling intensity on our results, as there were many more sites in KLB 9 (137 stations), compared to KLBs 7 and 8 (37 and 30 stations respectively). Sites exhibited spatial clustering (Fig. 1), so instead of random subsampling, we used a spatially explicit subsampling approach. Using the R package tidysdm (Leonardi et al., 2024), we spatially thinned our sites, with 10 replicates at each level of thinning. Sites were removed within a given radius of each station, so during the thinning process, the minimum distance between any two sites would be (i) 30 m, (ii) 50 m, and (iii) 70 m apart (Supplementary Fig. S3). We reassessed rarefaction curves for these thinned draws (Supplementary Fig. S4) and performed ecological analyses on both raw and thinned data.

Our methods account for Type II errors at the time of fossil collection. If taxa were actually present in the field but not collected or recorded (for whatever reason), we would have expected non-significant coherence, as coherence is determined by an over-abundance of shared embedded absences, which deviate significantly from null values (Leibold and Mikkelson, 2002). In such instances, the follow-up metrics of turnover and boundary clumping would be inappropriate to calculate.

3. Results

3.1. Fossil data

Data from the benthic members of the Molluscan Allomembers came from 37 sites in KLB 7, with 29 families present, 30 sites in KLB 8, with 32 families present, and 137 sites in KLB 9, with 43 families present. Rarefaction analyses over 100 iterations (Supplementary Fig. S2) suggest that the total number of benthic families present in the Molluscan Units may be approximately 45 families, and at least 150 sampling stations may be necessary to appropriately capture the full extent of this richness. At 95 % coverage, 21 families were present in KLB 7, 21 families were present in KLB 8, and 25 families were present at KLB 9 (Supplementary Fig. S2 and Supplementary Table 1).

In KLB 7, the bivalve family Gryphaeidae was most common, occurring in 13 out of 37 sites, followed by Cucullaeidae bivalves (11/37 sites) and Fasciolariidae gastropods (11/37 sites). In KLB 8, Aporrhaidae gastropods were most common, occurring in 15 out of 30 sites, followed by Amberleyidae gastropods (13/30) and Cucullaeidae bivalves (13/30). In KLB 9, the most common families were the bivalves Gryphaeidae (39/143) and Trigoniidae (39/143), followed by Fasciolariidae (34/143) and Amberleyidae gastropods (34/143).

Occurrence matrices, ordinated by the taxonomic similarity of constituent families, showed no clear temporal trends, as can be seen for the mixture of KLBs throughout the reciprocally ordinated matrix (Fig. 3a) and the NMDS ordination plot (Fig. 3b). Two KLB 9 sites fall outside the plotted NMDS axis limits but were included in the analyses. NMDS ordination yielded a stress of 0.069, indicating a good representation of the pairwise distances in two dimensions (Fig. 3b).

3.2. Pairwise analyses

3.2.1. Raw data

After removing singletons, 20 families were analysed in KLB 7, 20 families in KLB 8, and 35 families in KLB 9 (Supplementary Table 1). Significant non-random aggregations were seen among the sites in KLBs 7, 8, and 9. In KLB 7, 8.2 % of 73 analysed pairs displayed significant aggregations with each other (Fig. 4). Cucullaeidae bivalves were the only group to have more than 1 positively associated pair: they preferentially occurred with Veneridae bivalves and Fasciolariidae gastropods.

In KLB 8, the percentage of non-random aggregations increased slightly to 9.9 % among 91 analysed pairs (Fig. 4). Cucullaeidae, Hiatellidae, Trigoniidae bivalves and Amberleyidae, Cassidae, and Taiomidae gastropods each had 2 other taxa they were positively associated with.

In KLB 9, significant non-random associations were seen among 24.9 % of the 173 taxon pairs analysed (Fig. 4). Amberleyidae gastropods preferentially occurred with 9 other families, Aporrhaidae gastropods and Lahillidae bivalves had associations with 8 other families, and Perissityidae gastropods with 7 other families. The bivalve families Gryphaeidae and Hiatellidae occurred together less often than expected by random chance, showing the only negative association (Fig. 4).

3.2.2. Sensitivity results

For each studied KLB (7, 8 and 9), we recalculated the pairwise co-occurrence frequencies when the KLB windows were shifted to the west, shifted to the east, and contracted (as per Section 2.4). The increasing percentage of non-random associations through time remains true regardless of analyses applied – the percentage of aggregations for KLB 7 remains between 6.7 and 12.2 %, for KLB 8, between 4.7 and 13 %, and for KLB 9, the percentage of non-random associations remains between 24.2 and 24.9 % when the KLB windows are modified (Fig. 5).

We also spatially thinned our data by 30 m, 50 m, and 70 m (as per Section 2.4) (Fig. 5). These results show that the near tripling in non-random aggregations in KLB 9, as compared to KLB 7 and 8, holds

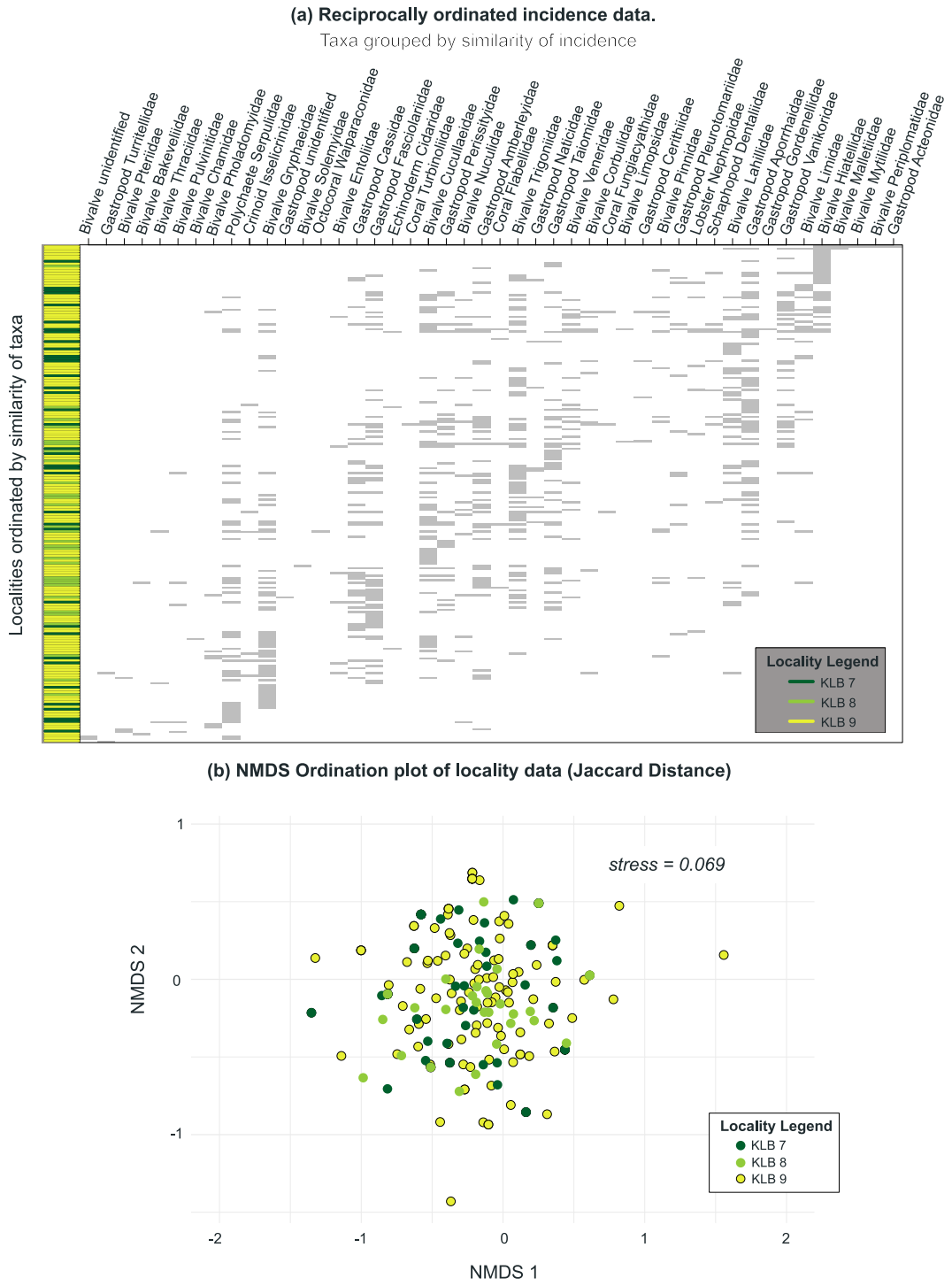

Fig. 3. (a) Incidence data per locality, reciprocally ordinated before plotting. Rows are localities in the study, coloured by KLB. Note that the KLB colours have been modified slightly from the geological map colours in Fig. 1, to aid in visual comparison. Localities are ordered by similarity of community composition. Columns are families in the study. Grey cells indicate presence, white cells indicate absence. No clear temporal trends are apparent based on the similarity of communities, i.e., localities on the y-axis do not group together by KLB and are instead interspersed together. (b) NMDS Ordination plot based on Jaccard dissimilarities on presence-absence data. Two KLB 9 sites fall outside the plotted axis limits and are not shown. Communities within the KLB units are largely the same, and no distinct clusters due to time are apparent.

true even at highest level of data pruning.

3.3. Metacommunity results

All our metacommunity results showed significant positive coherence (Table 3). Communities in KLB 7 resembled a nested clumped metacommunity (Fig. 6, Table 3), which is indicative of taxa-poor sites being subsets of larger taxa-pools (Table 1, Supplementary Fig. S1). In KLB 8, the metacommunity structure resembles that of a quasi-Clementsian one (quasi due to the non-significant turnover) (Fig. 6a, Table 3). Communities in KLB 9 resembled a Clementsian metacommunity structure (Fig. 6a, Table 3), which indicate that taxa are

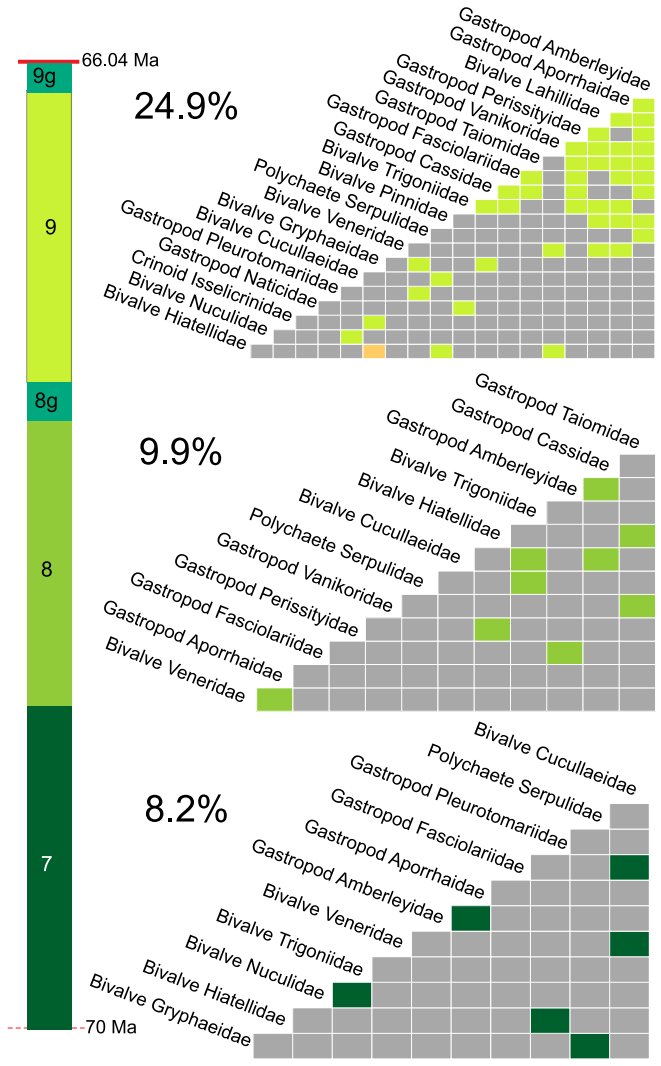

Fig. 4. The percentage of non-random aggregations between families in sites increases upsection. Positive associations are coloured in by the KLB colour number, as demonstrated in the scale bar. Negative associations are plotted in orange. Note that, to aid in visual comparison, the shades of green have been modified slightly from the accepted geological map colours in Fig. 1. (For interpretation of the references to colour in this figure legend, the reader is referred to the web version of this article.)

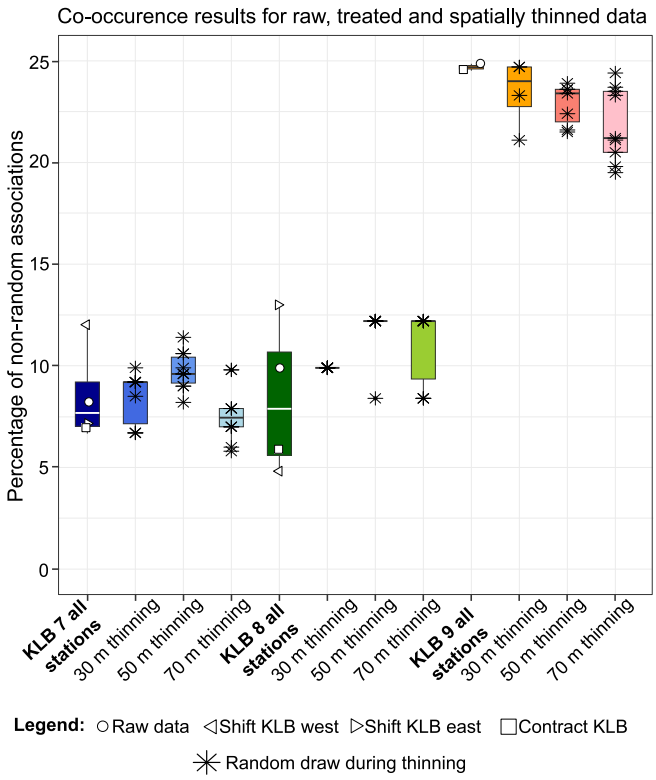

Fig. 5. Boxplots of the percentage of significant non-random associations in KLB 7 (blues), KLB 8 (greens) and KLB 9 (oranges/pinks). Jittered points show the results underlying the boxplots, and horizontal lines show the median. The first boxplot for each unit ("all stations") shows the results when positional boundaries are changed: circles are the raw data; left pointing arrows show the KLB west shift treatment; right pointing arrows show the KLB east shift treatment; squares show the contract KLB treatment. All other boxplots show results when KLBs are spatially thinned, and stars show the results from each random draw.

organized into distinct groups with high connectivity within them, and that groups of taxa change along the inferred gradient together due to strong environmental filtering (Table 1, Fig. S1).

When we applied our sensitivity analyses, we found that the informal cartographic unit KLB 7 had a nested clumped metacommunity structure when considering raw data, and when the width of the KLB was narrowed (Fig. 6a, Table 3). When the KLB window was shifted to the west or shifted to the east, i.e., when stratigraphically younger and older samples were incorporated, the metacommunity resembled a quasi Clementsian structure. For KLB 8, the metacommunities resembled weak quasi structures regardless of the sensitivity analyses (Fig. 6a, Table 3). Raw data, and shifting KLB 8 to the east and west, resembled quasi Clementsian structures. Contracting the KLB 8 window produced quasi nested clumped metacommunities. For KLB 9, strong Clementsian metacommunity structures were detected regardless of how the boundaries were defined (Fig. 6a, Table 3).

When the Molluscan units were spatially thinned (Fig. 6b), nested clumped metacommunities remained apparent in KLB 7, while the metacommunity structure in KLB 8 bridged the metacommunity structure between quasi nested clumped and quasi Clementsian, depending on random draws. Clementsian metacommunity structures were observed when KLB 9 was thinned by 30 m, with all ten random draws plotting in the non-nested space (Supplementary Fig. S6). With a thinning level of 50 m all draws resembled Clementsian metacommunities. When KLB 9 was thinned by 70 m, 4 random draws suggested Clementsian structures, while 6 draws suggested nested clumped structures (Fig. 6b).

4. Discussion

4.1. Spatiotemporal data advances

The thickness of the LBF, relatively uniform lithology, and evidence for deposition during changing sea levels and variable climate conditions, make Seymour Island a uniquely valuable site to study spatiotemporal ecosystem structure changes in the latest Cretaceous. A challenge for palaeoecological studies is the synthesis of historical fossil collections that were sampled opportunistically rather than systematically, with inconsistent sampling effort and absence of data tied accurately to measured sections. On Seymour Island one key difficulty with comparative analyses between fossil datasets is the cartographic positions of the KLB boundaries, which have proved challenging to identify in the field due to lithological homogeneity (Bowman et al., 2012). This uncertainty, together with subsequent taxonomic changes (Beu, 2009; Crame et al., 2014; Witts et al., 2015, 2016) and some stratigraphic ambiguity in the location of sampling stations (Crame et al., 2014) had previously hindered utility of the Zinsmeister Collection.

Table 3
Results from the Elements of Metacommunity Structure analyses. Note that negative *Z*-scores for coherence mean fewer embedded absences were observed than expected through chance, i.e., the coherence is positive. The significance of turnover is determined through its *p*-value; significant results ($p < 0.05$) are highlighted in bold.

KLB data treatment	Coherence (along a latent environmental gradient)		Turnover (along a latent environmental gradient)			Boundary Clumping (along a latent environmental gradient)		Inferred Meta-community structure
	Z-score	Interpretation	Z-score	Interpretation	*p* value	Morisita's Index	Interpretation	
KLB 7 raw	−4.49:	Taxa respond synchronously to the environmental gradient	−2.03: Taxa's ranges are nested	Taxa loss without replacement	**0.04**	2.5	Multiple taxa have ranges that end in the same positions	Nested clumped
KLB 7 west shift	−7.26	Taxa respond synchronously to the environmental gradient	0.64: Taxa's ranges are non-nested	Active replacement of taxa	0.52	3.5	Multiple taxa have ranges that end in the same positions	Quasi-Clementsian
KLB 7 east shift	−7.98	Taxa respond synchronously to the environmental gradient	0.37: Taxa's ranges are non-nested	Active replacement of taxa	0.71	3.3	Multiple taxa have ranges that end in the same positions	Quasi-Clementsian
KLB 7 contracted	−2.49:	Taxa respond synchronously to the environmental gradient	−2.60 Taxa's ranges are nested	Taxa loss without replacement	**0.009**	2.4	Multiple taxa have ranges that end in the same positions	Nested clumped
KLB 8 raw	−6.47:	Taxa respond synchronously to the environmental gradient	0.14: Taxa's ranges are non-nested	Active replacement of taxa	0.89	3.4	Multiple taxa have ranges that end in the same positions	Quasi-Clementsian
KLB 8 west shift	−5.70	Taxa respond synchronously to the environmental gradient	0.32 Taxa's ranges are non-nested	Active replacement of taxa	0.75	2.6	Multiple taxa have ranges that end in the same positions	Quasi-Clementsian
KLB 8 east shift	−9.98	Taxa respond synchronously to the environmental gradient	0.27 Taxa's ranges are non-nested	Active replacement of taxa	0.78	1.9	Multiple taxa have ranges that end in the same positions	Quasi-Clementsian
KLB 8 contracted	−5.16	Taxa respond synchronously to the environmental gradient	−1.15 Taxa's ranges are non-nested	Taxa loss without replacement	0.25	3.2	Multiple taxa have ranges that end in the same positions	Quasi- Nested clumped
KLB 9 raw	−8.46	Taxa respond synchronously to the environmental gradient	2.99 Taxa's ranges are non-nested	Active replacement of taxa	**0.003**	2.7	Multiple taxa have ranges that end in the same positions	Clementsian
KLB 9 contracted	−8.09	Taxa respond synchronously to the environmental gradient	2.83 Taxa's ranges are non-nested	Active replacement of taxa	**0.004**	3.1	Multiple taxa have ranges that end in the same positions	Clementsian

In this study we developed a novel approach to dealing with the spatial uncertainty, namely sensitivity analyses around the KLB boundaries, and so are now able to test whether these positional uncertainties affect ecological results, as well as testing the impact of differential sampling intensity through our spatial thinning analyses. All sensitivity analyses demonstrated that ecological analyses of taxonomic pairs are robust to variations in subsets of data (c.f. Veech, 2013) (Fig. 5), consistently showing a near tripling of non-random associations between taxa pairs up-section. Any possible Type II errors in the underlying data did not influence our metacommunity results, as all our results showed significant positive coherence, however, our analyses at the metacommunity level are more sensitive to subsampling. When data are strongly thinned by 70 m in KLB 9, notably reducing the spatial aggregations of stations and the number of stations (from 137 to 59, Supplementary Fig. S3), this reduction results in turnover metrics that are more negative, placing metacommunities in the nested, rather than non-nested space. The resulting nested clumped metacommunity structure, rather than a Clementsian one, make taxa-poor sites appear as subsets of taxa-rich sites – a likely sampling artifact. This change in metacommunity structure contrasts with no significant change between KLB 7 and KLB 8 (Fig. 6), where the strongest thinning (70 m) removed only 6 stations in KLB 7 and 1 station in KLB 8. These results suggest that we should not be drawing strong conclusions from our metacommunity analyses in terms of differences between the KLB units but can do so for our co-occurrence analyses. These sensitivity analyses highlight the importance of even sampling effort (wherever possible), both spatially as well as stratigraphically, in order to limit influence of sampling biases. Despite these caveats, our sensitivity analyses allow us to fully utilize spatial data from the PRI Zinsmeister collection to study ecological complexity.

4.2. Ecological complexity

Sites within our study, when ordinated by similarities in community composition, display no temporal trends (Fig. 3a), suggesting no notable taxonomic turnover over the ~4 million years covered by our analyses. Instead, there is only an increase in standing richness at the family level in KLB 9 (Table 2, Supplementary Fig. S1, Supplementary Table 1). Traditional methods of ordination, such as NMDS (Fig. 3b) shows substantial overlap among the KLB 7, 8, and 9 sites, suggesting broadly similar communities over the ~4 million years. However, this approach fails to capture the internal metacommunity structures that exist within this data, and so that ecological complexity, i.e., the tendency for taxa to preferentially aggregate or segregate due to biotic interactions or environmental filtering, has increased through time. Our co-occurrence analyses show a dramatic increase in the percentage of non-random pairwise co-occurrences in KLB 9. These patterns are consistent even when spatially subsampling the data (Fig. 5). The increase in the non-

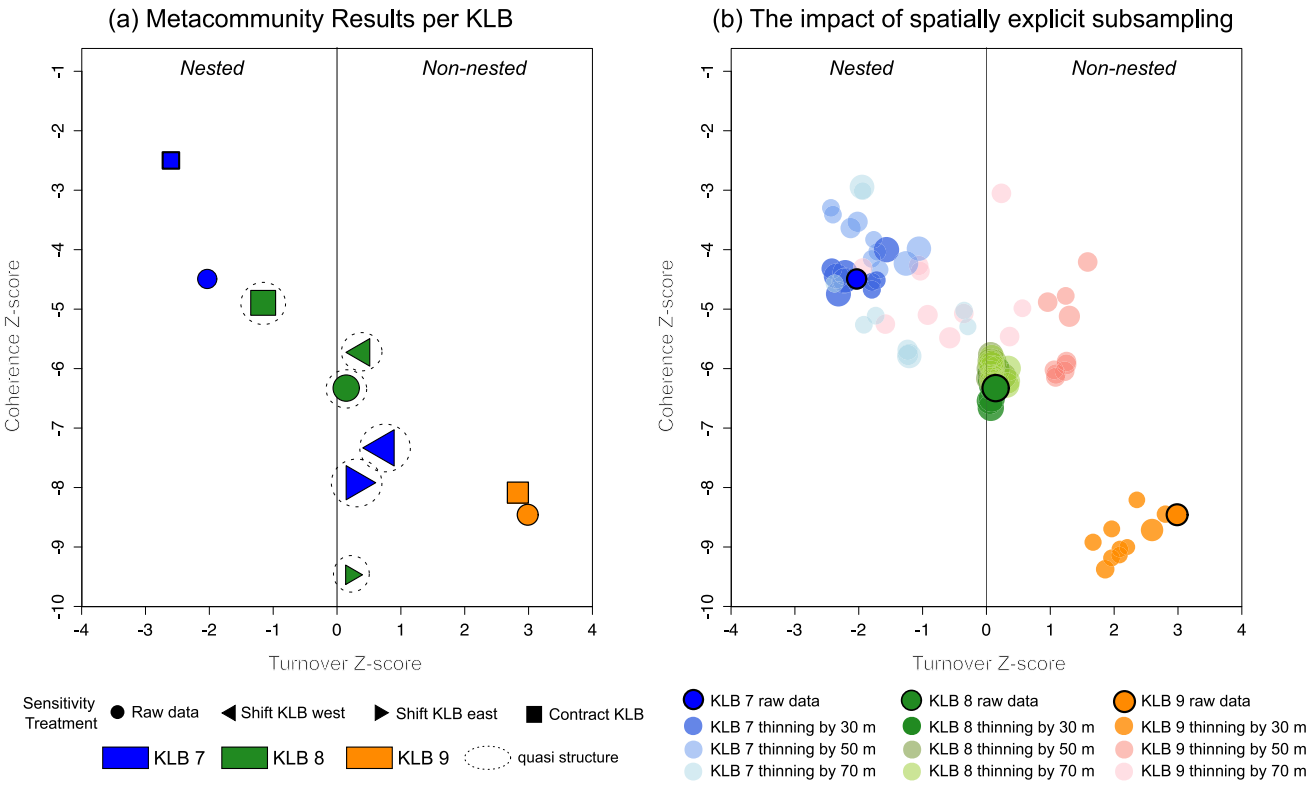

Fig. 6. **(a)** Metacommunity results across the LBF Molluscan units. Raw data is noted with circles, treated data are marked with the relevant symbols. Circles are the raw data; left pointing arrows show the KLB west shift treatment; right pointing arrows show the KLB east shift treatment; squares show the contract KLB treatment. Quasi structures (with non-significant turnover) are outlined with dotted rings, while significant structures do not have rings. The size of the symbol is proportional to Morisita's Index, which reflects the degree of boundary clumping. (b) Metacommunity results when the raw data are spatially thinned by 30 m, 50 m and 70 m. The raw results are highlighted with solid black outlines.

random associations of the gastropods Amberleyidae, Aporrhaidae and Perissityidae and Lahillidae bivalves between KLBs 7 and 8 relative to KLB 9 shows that these families are increasingly found together, possibly reflecting shared habitat preferences and that they may play a stronger role in defining community composition in KLB 9. Further evidence of increased ecological complexity in KLB 9 comes from the only negative association detected between deep infaunal Hiatellidae and epifaunal Gryphaeidae bivalves. This negative association may reflect differing responses to events like sediment disturbance consistent with Thayer's 'biological bulldozer' scenario (Thayer, 1979) and highlighting more nuanced, indirect community interactions. Importantly, differential levels of sampling, as evidenced by rarefaction curves, show that this near three-fold increase in non-random associations in KLB 9 (Fig. 5), is not a result of more extensive sampling in this unit, but rather a true ecological pattern.

At the metacommunity level, we note a shift in taxonomic turnover from nestedness in KLB 7 to replacement in KLB 9 (Fig. 6), which also corresponds to an increase in complexity, as replacement is a consequence of environmental sorting or biotic interactions, whereas nestedness reflect subsets (Baselga, 2010). However, our metacommunity results are not as strong as our pairwise patterns. While the raw data record the increase in taxa replacement from KLB 7 to KLB 9, these results are not robust to strong spatial thinning, so it is not possible to conclude whether the change to a Clementsian structure from a nested clumped metacommunity structure is a true signal, or one brought on through clustered sampling sites. Although KLB 7 and 8 are well sampled in terms of taxonomic richness (Supplementary Fig. S2, S4, and Supplementary Table 1), the limited number of sites may prevent us from confidently resolving their metacommunity structures. Note though, the significant increase in co-occurrences (Figs. 4 and 5) is consistent with an increase in metacommunity complexity, suggesting we may be picking up on a subtle signal, while not being able to draw any firm conclusions.

4.3. Pattern of K–Pg extinction in Antarctica

Our complexity results can be used to investigate the competing hypotheses about the nature of the K–Pg extinction in Antarctica, as complexity correlates to ecosystem resilience (Pimm, 1984). If the extinction was gradual, induced by global climatic changes or longer-term changes in ocean chemistry during the time interval represented by the uppermost ~50 m of KLB 9 (Zinsmeister et al., 1989; Zinsmeister, 1998), then both the percentage of non-random associations, as well as turnover, should decrease due to species loss (Wright et al., 1998). With localities not tied to section lines (see Methods), we can assess the patterns only at the whole KLB level. Our sensitivity tests show that even with spatial thinning, non-random associations in KLB 9 are consistently higher than in KLB 7 and KLB 8. The possible increase in metacommunity complexity (as inferred through increasing turnover), with an almost tripling of non-random associations, is not consistent with a drawn-out or gradual extinction through KLB 9.

Considering a multi-phased extinction, with a precursor extinction coincident with the late Maastrichtian climate warming associated with Deccan Trap volcanism (Tobin et al., 2012; Schoene et al., 2019; Sprain et al., 2019; Hull et al., 2020), would presumably place at least part of the terminal KLB 9 unit in a post-extinction phase with significant negative turnover (Wright et al., 1998). These post-extinction communities would likely also show an increase in generalists with a decrease in specialists (Erwin, 1998), which is contrary to the increase in significant non-random pairwise co-occurrences, which indicate an increase in specialization. As such, a precursor extinction seems unlikely, although due to sampling constraints we cannot test this directly (see

Methods 2.4).

5. Conclusions

Our work capitalizes on the exceptional and expanded outcrop of onshore Cretaceous–Paleogene sedimentary successions found in Seymour Island, Antarctic Peninsula, to study ecological patterns leading up to the Cretaceous-Paleogene (K–Pg) mass extinction. We found no clear temporal trends in taxonomic turnover across KLBs 7–9, suggesting ecological rather than evolutionary drivers of community structure. We discovered a notable increase in ecological complexity, reflected in both significantly non-random co-occurrences among benthic taxa, and the transition from nested clumped to more specialized Clementsian metacommunity structures. Although sensitivity tests suggest changes in metacommunity structures may be influenced by uneven sampling intensity, our finding of increasing specialization and complexity does not support gradual declines in biodiversity prior to the K–Pg event, instead supporting a single, catastrophic mass extinction in Antarctica. Moving forward, resolving uncertainties in stratigraphic positions, improving sample coverage, and incorporating higher taxonomic resolution, i.e., at species level, would allow finer-scale ecological signals to be detected. Integrating measures of functional morphological diversity, along with additional palaeoenvironmental data, would help clarify the ecological roles and niche structures of these communities. Finally, applying the same ecological complexity framework to other K–Pg boundary sections worldwide could test whether the rise in community complexity documented at Seymour Island also occurred in other marine ecosystems, or whether it reflects ecological dynamics specific to the Antarctic region.

CRediT authorship contribution statement

Tasnuva Ming Khan: Writing – review & editing, Writing – original draft, Visualization, Methodology, Investigation, Funding acquisition, Formal analysis, Data curation, Conceptualization. **Rowan J. Whittle:** Writing – review & editing, Supervision, Methodology, Data curation, Conceptualization. **James D. Witts:** Writing – review & editing, Resources, Investigation, Data curation. **Huw J. Griffiths:** Writing – review & editing, Supervision, Methodology, Conceptualization. **Andrea Manica:** Writing – review & editing, Supervision, Methodology, Conceptualization. **Emily G. Mitchell:** Writing – review & editing, Supervision, Methodology, Funding acquisition, Formal analysis, Conceptualization.

Funding

This work has been supported by Natural Environment Research Council (NERC) Independent Research Fellowship NE/S014756/1, awarded to EM. TMK is funded by a Cambridge International and Newnham College Scholarship, administered by Cambridge Trust. The Newnham College United States Travel Bursary funded TMK's visit to the PRI Collections. RJW and HJG are funded by UK Research and Innovation (UKRI) Future Leaders Fellowship MR/W01002X/1 "The past, present and future of unique cold-water benthic (seafloor) ecosystems in the Southern Ocean" awarded to RJW. HJG is also funded by BIOPOLE, under the National Capability Science Multi-Centre award scheme (NC-SM2).

Declaration of competing interest

The authors declare no competing interests.

Acknowledgements

We thank the Paleontological Research Institution, in particular Dr. Greg Dietl, Leslie Skibinski and Vicky Wang for providing access to the Zinsmeister Collection of Antarctic fossils, and their kind hospitality during TMK's stay. We thank Dr. Alex Dunhill, the editor, and two anonymous reviewers who provided feedback on earlier versions of this manuscript. TMK thanks Nile Stephenson for helpful discussions regarding sampling methods. TMK further thanks PRI Director Dr. Warren Allmon for introducing her to the field of palaeontology during her freshman year.

Appendix A. Supplementary data

Supplementary data to this article can be found online at https://doi.org/10.1016/j.palaeo.2025.113495.

Data availability

Occurrence data (at Family level) via the UK Polar Data Centre:

Khan, T.M., Whittle, R.J., Witts, J.D., Griffiths, H.J., Manica, A., & Mitchell, E.G. (2025). Invertebrate fossil occurrences from the Cretaceous López de Bertodano Formation (Maastrichtian), Seymour Island, housed in the Paleontological Research Institution (PRI), Ithaca, NY (Version 1.0) [Data set]. NERC EDS UK Polar Data Centre. https://doi.org/10.5285/c1252fb5-8075-431c-a78b-1c1d8da37c5e

All code used in this study can be found via Zenodo: https://doi.org/10.5281/zenodo.17816575

References

Aberhan, M., Kiessling, W., 2015. Persistent ecological shifts in marine molluscan assemblages across the end-cretaceous mass extinction. Proc. Natl. Acad. Sci. 112, 7207–7212. https://doi.org/10.1073/pnas.1422248112.

Acosta Hospitaleche, C., Jones, W., 2024. Were terror birds the apex continental predators of Antarctica? New findings in the early Eocene of Seymour Island. Palaeontol. Electron. https://doi.org/10.26879/1340.

Allen, M.R., VanDyke, J.N., Cáceres, C.E., 2011. Metacommunity assembly and sorting in newly formed lake communities. Ecology 92, 269–275. https://doi.org/10.1890/10-0522.1.

Anderson, J.B., Warny, S., Askin, R.A., Wellner, J.S., Bohaty, S.M., Kirshner, A.E., Livsey, D.N., Simms, A.R., Smith, T.R., Ehrmann, W., Lawver, L.A., Barbeau, D., Wise, S.W., Kulhanek, D.K., Weaver, F.M., Majewski, W., 2011. Progressive Cenozoic cooling and the demise of Antarctica's last refugium. Proc. Natl. Acad. Sci. 108, 11356–11360. https://doi.org/10.1073/pnas.1014885108.

Aronson, R.B., Blake, D.B., 2001. Global climate change and the origin of modern benthic communities in Antarctica. Am. Zool. 41, 27–39. https://doi.org/10.1093/icb/41.1.27.

Aronson, R.B., Blake, D.B., Oji, T., 1997. Retrograde community structure in the late Eocene of Antarctica. Geology 25, 903. https://doi.org/10.1130/0091-7613(1997)025%253C0903:RCSITL%253E2.3.CO;2.

Askin, R.A., 1988. Campanian to Paleocene palynological succession of Seymour and adjacent islands, northeastern Antarctic Peninsula. Geol. Soc. Am. Mem. 169, 131–154. https://doi.org/10.1130/mem169-p131.

Bambach, R.K., 2006. Phanerozoic biodiversity: mass extinctions. Annu. Rev. Earth Planet. Sci. 34, 127–155. https://doi.org/10.1146/annurev.earth.33.092203.122654.

Barnet, J.S.K., Littler, K., Kroon, D., Leng, M.J., Westerhold, T., Röhl, U., Zachos, J.C., 2018. A new high-resolution chronology for the late Maastrichtian warming event: establishing robust temporal links with the onset of Deccan volcanism. Geology 46, 147–150. https://doi.org/10.1130/G39771.1.

Barreda, V.D., Palazzesi, L., Tellería, M.C., Olivero, E.B., Raine, J.I., Forest, F., 2015. Early evolution of the angiosperm clade Asteraceae in the cretaceous of Antarctica. Proc. Natl. Acad. Sci. 112, 10989–10994. https://doi.org/10.1073/pnas.1423653112.

Baselga, A., 2010. Partitioning the turnover and nestedness components of beta diversity: partitioning beta diversity. Glob. Ecol. Biogeogr. 19, 134–143. https://doi.org/10.1111/j.1466-8238.2009.00490.x.

Beu, A.G., 2009. Before the ice: biogeography of Antarctic paleogene molluscan faunas. Palaeogeogr. Palaeoclimatol. Palaeoecol. 284, 191–226. https://doi.org/10.1016/j.palaeo.2009.09.025.

Blanchet, F.G., Cazelles, K., Gravel, D., 2020. Co-occurrence is not evidence of ecological interactions. Ecol. Lett. 23, 1050–1063. https://doi.org/10.1111/ele.13525.

Bowman, V.C., Francis, J.E., Riding, J.B., Hunter, S.J., Haywood, A.M., 2012. A latest cretaceous to earliest Paleogene dinoflagellate cyst zonation from Antarctica, and implications for phytoprovincialism in the high southern latitudes. Rev. Palaeobot. Palynol. 171, 40–56. https://doi.org/10.1016/j.revpalbo.2011.11.004.

Bowman, V.C., Francis, J.E., Riding, J.B., 2013. Late cretaceous winter sea ice in Antarctica? Geology 41, 1227–1230. https://doi.org/10.1130/G34891.1.

Bown, P., 2005. Selective Calcareous Nannoplankton Survivorship at the Cretaceous-Tertiary Boundary.

Brecher, H.H., Tope, R.W., 1988. Topographic map of Seymour Island. In: Feldmann, R. M., Woodburne, M.O. (Eds.), Geology and Paleontology of Seymour Island Antarctic Peninsula, Memoirs. Geol. Soc. Am, pp. 17–20. https://doi.org/10.1130/MEM169.
Brusatte, Stephen L., Butler, R.J., Barrett, P.M., Carrano, M.T., Evans, D.C., Lloyd, G.T., Mannion, P.D., Norell, M.A., Peppe, D.J., Upchurch, P., Williamson, T.E., 2015a. The extinction of the dinosaurs. Biol. Rev. 90, 628–642. https://doi.org/10.1111/brv.12128.
Brusatte, Stephen L., O'Connor, J.K., Jarvis, E.D., 2015b. The Origin and diversification of Birds. Curr. Biol. 25, R888–R898. https://doi.org/10.1016/j.cub.2015.08.003.
Case, J.A., 1988. Paleogene floras from Seymour Island, Antarctic Peninsula. Geol. Soc. Am. Mem. 169, 523–540. https://doi.org/10.1130/mem169-p523.
Case, J.A., Woodburne, M.O., Chaney, D.S., 1988. A new genus of polydolopid marsupial from Antarctica. Geol. Soc. Am. Mem. 169, 505–522. https://doi.org/10.1130/mem169-p505.
Chao, A., Gotelli, N.J., Hsieh, T.C., Sander, E.L., Ma, K.H., Colwell, R.K., Ellison, A.M., 2014. Rarefaction and extrapolation with Hill numbers: a framework for sampling and estimation in species diversity studies. Ecol. Monogr. 84, 45–67. https://doi.org/10.1890/13-0133.1.
Collins, M.D., Simberloff, D., Connor, E.F., 2011. Binary matrices and checkerboard distributions of birds in the Bismarck Archipelago: bismarck Archipelago birds. J. Biogeogr. 38, 2373–2383. https://doi.org/10.1111/j.1365-2699.2011.02506.x.
Cottenie, K., De Meester, L., 2003. Connectivity and cladoceran species richness in a metacommunity of shallow lakes. Freshw. Biol. 48, 823–832. https://doi.org/10.1046/j.1365-2427.2003.01050.x.
Crame, J.A., 2019. Paleobiological significance of the James Ross Basin, p. 30.
Crame, J.A., Francis, J.E., Cantrill, D.J., Pirrie, D., 2004. Maastrichtian stratigraphy of Antarctica. Cretac. Res. 25, 411–423. https://doi.org/10.1016/j.cretres.2004.02.002.
Crame, J.A., Beu, A.G., Ineson, J.R., Francis, J.E., Whittle, R.J., Bowman, V.C., 2014. The early origin of the antarctic marine fauna and its evolutionary implications. PLoS One 9, e114743. https://doi.org/10.1371/journal.pone.0114743.
Dallas, T., 2014. Metacom: an R package for the analysis of metacommunity structure. Ecography 37, 402–405. https://doi.org/10.1111/j.1600-0587.2013.00695.x.
Datry, T., Bonada, N., Heino, J., 2016. Towards understanding the organisation of metacommunities in highly dynamic ecological systems. Oikos 125, 149–159. https://doi.org/10.1111/oik.02922.
Diamond, J.M., 1975. Assembly of species communities. In: Diamond, J.M., Cody, M.L. (Eds.), Ecology and Evolution of Communities. Harvard University Press, Boston, pp. 342–344.
Dietl, G.P., 2010. Spotlight on collections: the zinsmeister collection. Am. Paleontol. 18.
Douglas, P.M.J., Affek, H.P., Ivany, L.C., Houben, A.J.P., Sijp, W.P., Sluijs, A., Schouten, S., Pagani, M., 2014. Pronounced zonal heterogeneity in Eocene southern high-latitude sea surface temperatures. Proc. Natl. Acad. Sci. 111, 6582–6587. https://doi.org/10.1073/pnas.1321441111.
Eden, R., Manica, A., Mitchell, E.G., 2022. Metacommunity analyses show an increase in ecological specialisation throughout the Ediacaran period. PLoS Biol. 20, e3001289. https://doi.org/10.1371/journal.pbio.3001289.
Edie, S.M., Jablonski, D., Valentine, J.W., 2018. Contrasting responses of functional diversity to major losses in taxonomic diversity. Proc. Natl. Acad. Sci. 115, 732–737. https://doi.org/10.1073/pnas.1717636115.
Edie, S.M., Collins, K.S., Jablonski, D., 2025. The end-cretaceous mass extinction restructured functional diversity but failed to configure the modern marine biota. Sci. Adv. 11 (21), eadv1171. https://doi.org/10.1126/sciadv.adv1171.
Elliot, D.H., Askin, R.A., Kyte, F.T., Zinsmeister, W.J., 1994. Iridium and dinocysts at the cretaceous-tertiary boundary on Seymour Island, Antarctica: implications for the K-T event. Geology 22, 675. https://doi.org/10.1130/0091-7613(1994)022%253C0675:IADATC%253E2.3.CO;2.
Erwin, D.H., 1998. The end and the beginning: recoveries from mass extinctions. Trends Ecol. Evol. 13, 344–349. https://doi.org/10.1016/S0169-5347(98)01436-0.
Ferreira Da Silva, L.C., Santos, A., Fauth, G., Manríquez, L.M.E., Kochhann, K.G.D., Guerra, R.D.M., Horodyski, R.S., Villegas-Martín, J., Ribeiro Da Silva, R., 2023. High-latitude cretaceous–Paleogene transition: new paleoenvironmental and paleoclimatic insights from Seymour Island, Antarctica. Mar. Micropaleontol. 180, 102214. https://doi.org/10.1016/j.marmicro.2023.102214.
Field, D.J., Bercovici, A., Berv, J.S., Dunn, R., Fastovsky, D.E., Lyson, T.R., Vajda, V., Gauthier, J.A., 2018. Early evolution of modern birds structured by global forest collapse at the end-cretaceous mass extinction. Curr. Biol. 28, 1825–1831.e2. https://doi.org/10.1016/j.cub.2018.04.062.
Flannery-Sutherland, J.T., Crossan, C.D., Myers, C.E., Hendy, A.J.W., Landman, N.H., Witts, J.D., 2024. Late cretaceous ammonoids show that drivers of diversification are regionally heterogeneous. Nat. Commun. 15, 5382. https://doi.org/10.1038/s41467-024-49462-z.
Francis, J.E., Crame, J.A., Pirrie, D., 2006. Cretaceous-Tertiary high-latitude palaeoenvironments, James Ross Basin, Antarctica: introduction. Geol. Soc. Lond. Spec. Publ. 258, 1–5. https://doi.org/10.1144/GSL.SP.2006.258.01.01.
Gallala, N., Zaghbib-Turki, D., Arenillas, I., Arz, J.A., Molina, E., 2009. Catastrophic mass extinction and assemblage evolution in planktic foraminifera across the cretaceous/Paleogene (K/Pg) boundary at Bidart (SW France). Mar. Micropaleontol. 72, 196–209. https://doi.org/10.1016/j.marmicro.2009.05.001.
García-Girón, J., Heino, J., Alahuhta, J., Chiarenza, A.A., Brusatte, S.L., 2021. Palaeontology meets metacommunity ecology: the Maastrichtian dinosaur fossil record of North America as a case study. Palaeontology 64, 335–357. https://doi.org/10.1111/pala.12526.
Gauch, H.G., Whittaker, R.H., Wentworth, T.R., 1977. A comparative study of reciprocal averaging and other ordination techniques. J. Ecol. 65, 157. https://doi.org/10.2307/2259071.
Green, W.A., Hunt, G., Wing, S.L., DiMichele, W.A., 2011. Does extinction wield an axe or pruning shears? How interactions between phylogeny and ecology affect patterns of extinction. Paleobiology 37, 72–91. https://doi.org/10.1666/09078.1.
Griffith, D.M., Veech, J.A., Marsh, C.J., 2016. Cooccur: probabilistic species co-occurrence analysis in *R*. J. Stat. Softw. 69. https://doi.org/10.18637/jss.v069.c02.
Grossnickle, D.M., Newham, E., 2016. Therian mammals experience an ecomorphological radiation during the Late Cretaceous and selective extinction at the K–Pg boundary. Proc. R. Soc. B Biol. Sci. 283, 20160256. https://doi.org/10.1098/rspb.2016.0256.
Hathway, B., 2000. Continental rift to back-arc basin: Jurassic–Cretaceous stratigraphical and structural evolution of the Larsen Basin, Antarctic Peninsula. J. Geol. Soc. Lond. 157, 417–432. https://doi.org/10.1144/jgs.157.2.417.
Heino, J., 2005. Metacommunity patterns of highly diverse stream midges: gradients, chequerboards, and nestedness, or is there only randomness? Ecol. Entomol. 30, 590–599. https://doi.org/10.1111/j.0307-6946.2005.00728.x.
Heino, J., Melo, A.S., Siqueira, T., Soininen, J., Valanko, S., Bini, L.M., 2015a. Metacommunity organisation, spatial extent and dispersal in aquatic systems: patterns, processes and prospects. Freshw. Biol. 60, 845–869. https://doi.org/10.1111/fwb.12533.
Heino, J., Nokela, T., Soininen, J., Tolkkinen, M., Virtanen, L., Virtanen, R., 2015b. Elements of metacommunity structure and community-environment relationships in stream organisms. Freshw. Biol. 60, 973–988. https://doi.org/10.1111/fwb.12556.
Heino, J., Soininen, J., Alahuhta, J., Lappalainen, J., Virtanen, R., 2015c. A comparative analysis of metacommunity types in the freshwater realm. Ecol. Evol. 5, 1525–1537. https://doi.org/10.1002/ece3.1460.
Hsieh, T.C., Ma, K.H., Chao, A., 2024. iNEXT: Interpolation and Extrapolation for Species Diversity.
Hull, P., 2015. Life in the aftermath of mass extinctions. Curr. Biol. 25, R941–R952. https://doi.org/10.1016/j.cub.2015.08.053.
Hull, P.M., Bornemann, A., Penman, D.E., Henehan, M.J., Norris, R.D., Wilson, P.A., Blum, P., Alegret, L., Batenburg, S.J., Bown, P.R., Bralower, T.J., Cournede, C., Deutsch, A., Donner, B., Friedrich, O., Jehle, S., Kim, H., Kroon, D., Lippert, P.C., Loroch, D., Moebius, I., Moriya, K., Peppe, D.J., Ravizza, G.E., Röhl, U., Schueth, J. D., Sepúlveda, J., Sexton, P.F., Sibert, E.C., Śliwińska, K.K., Summons, R.E., Thomas, E., Westerhold, T., Whiteside, J.H., Yamaguchi, T., Zachos, J.C., 2020. On impact and volcanism across the Cretaceous-Paleogene boundary. Science 367, 266–272. https://doi.org/10.1126/science.aay5055.
Jadwiszczak, P., 2006. Eocene penguins of Seymour Island, Antarctica: the earliest record, taxonomic problems and some evolutionary considerations. Pol. Polar Res. 27.
Khan, T.M., Whittle, R.J., Witts, J., Griffiths, H.J., Manica, A., Mitchell, E.G., 2025a. Lbf-Complexity: Code for Khan et al. (2025) Metacommunity Structural Changes of Antarctic Benthic Invertebrates Over the Late Maastrichtian. https://doi.org/10.5281/zenodo.17816575.
Khan, T.M., Whittle, R.J., Witts, J.D., Griffiths, H.J., Manica, A., Mitchell, E.G., 2025b. [Data set] Invertebrate Fossil Occurrences From the Cretaceous Lopez de Bertodano Formation (Maastrichtian), Seymour Island, Housed in the Paleontological Research Institution (PRI), Ithaca, NY. (Version 1.0). NERC EDS UK Polar Data Centre. https://doi.org/10.5285/c1252fb5-8075-431c-a78b-1c1d8da37c5e.
Klompmaker, A.A., Finnegan, S., 2018. Extreme rarity of competitive exclusion in modern and fossil marine benthic ecosystems. Geology 46, 723–726. https://doi.org/10.1130/G45032.1.
Leibold, M.A., Mikkelson, G.M., 2002. Coherence, species turnover, and boundary clumping: elements of meta-community structure. Oikos 97, 237–250. https://doi.org/10.1034/j.1600-0706.2002.970210.x.
Leibold, M.A., Holyoak, M., Mouquet, N., Amarasekare, P., Chase, J.M., Hoopes, M.F., Holt, R.D., Shurin, J.B., Law, R., Tilman, D., Loreau, M., Gonzalez, A., 2004. The metacommunity concept: a framework for multi-scale community ecology. Ecol. Lett. 7, 601–613. https://doi.org/10.1111/j.1461-0248.2004.00608.x.
Leonardi, M., Colucci, M., Pozzi, A.V., Scerri, E.M.L., Manica, A., 2024. Tidysdm: Species distribution Models With Tidymodels.
Little, C.T.S., Birgel, D., Boyce, A.J., Crame, J.A., Francis, J.E., Kiel, S., Peckmann, J., Pirrie, D., Rollinson, G.K., Witts, J.D., 2015. Late cretaceous (Maastrichtian) shallow water hydrocarbon seeps from Snow Hill and Seymour Islands, James Ross Basin, Antarctica. Palaeogeogr. Palaeoclimatol. Palaeoecol. 418, 213–228. https://doi.org/10.1016/j.palaeo.2014.11.020.
Logue, J.B., Mouquet, N., Peter, H., Hillebrand, H., 2011. Empirical approaches to metacommunities: a review and comparison with theory. Trends Ecol. Evol. 26, 482–491. https://doi.org/10.1016/j.tree.2011.04.009.
Macellari, C.E., 1984. Late Cretaceous Stratigraphy, Sedimentology, and Macropaleontology of Seymour Island, Antarctic Peninsula (Doctoral dissertation).. Ohio State University.
Macellari, C.E., 1988. Stratigraphy, Sedimentology, and Paleoecology of Upper Cretaceous/Paleocene Shelf-Deltaic Sediments of Seymour Island, Geological Society of America Memoirs. Geological Society of America, pp. 25–54. https://doi.org/10.1130/MEM169-p25.
Marshall, C.R., 1995. Distinguishing between sudden and gradual extinctions in the fossil record: predicting the position of the Cretaceous-Tertiary iridium anomaly using the ammonite fossil record on Seymour Island, Antarctica. Geology 23, 731. https://doi.org/10.1130/0091-7613(1995)023%253C0731:dbsage%253E2.3.co;2.
Marshall, C.R., Finnegan, S., Clites, E.C., Holroyd, P.A., Bonuso, N., Cortez, C., Davis, E., Dietl, G.P., Druckenmiller, P.S., Eng, R.C., Garcia, C., Estes-Smargiassi, K., Hendy, A., Hollis, K.A., Little, H., Nesbitt, E.A., Roopnarine, P., Skibinski, L., Vendetti, J., White, L.D., 2018. Quantifying the dark data in museum fossil collections as palaeontology undergoes a second digital revolution. Biol. Lett. 14, 20180431. https://doi.org/10.1098/rsbl.2018.0431.

McArthur, J.M., Thirlwall, M.F., Engkilde, M., Zinsmeister, W.J., Howarth, R.J., 1998. Strontium isotope profiles across K/T boundary sequences in Denmark and Antarctica. Earth Planet. Sci. Lett. 160, 179–192. https://doi.org/10.1016/S0012-821X(98)00058-2.

McArthur, J.M., Crame, J.A., Thirlwall, M.F., 2000. Definition of late cretaceous stage boundaries in Antarctica using strontium isotope stratigraphy. J. Geol. 108, 623–640. https://doi.org/10.1086/317952.

Molina, E., Alegret, L., Arenillas, I., Arz, J.A., Gallala, N., Hardenbol, J., von Salis, K., Steurbaut, E., Vandenberghe, N., Zaghbib-Turki, D., 2006. The global boundary stratotype section and point for the base of the Danian stage (paleocene, paleogene, "tertiary", cenozoic) at El Kef, Tunisia - Original definition and revision. Episodes J. Int. Geosci. 29, 263–273.

Montes, M., Beamud, E., Nozal, F., 2019a. Late Maastrichtian–Paleocene Chronostratigraphy From Seymour Island, James Ross Basin, Antarctic Peninsula: Eustatic Controls on Sedimentation, p. 30.

Montes, M., Nozal, F., Santillana, S.N., Marenssi, S., Olivero, E., 2019b. Mapa Geológico de la isla de Marambio (Seymour); escala 1:20.000. 1ºedición. Acompañado de mapas. Madrid-Instituto Geológico y Minero de España; Buenos Aires-Instituto Antártico Argentino, p. 250. Serie Cartográfica Geocientífica Antártica.

Morisita, M., 1962. Iσ-Index, a measure of dispersion of individuals. Res. Popul. Ecol. 4, 1–7. https://doi.org/10.1007/BF02533903.

Nicholson, T.D., 1991. Preserving the Earth's biological diversity: the role of museums. Curator Mus. J. 34, 85–108. https://doi.org/10.1111/j.2151-6952.1991.tb01458.x.

Odling-Smee, J., Erwin, D.H., Palkovacs, E.P., Feldman, M.W., Laland, K.N., 2013. Niche construction theory: a practical guide for ecologists. Q. Rev. Biol. 88, 3–28. https://doi.org/10.1086/669266.

Oksanen, J., Simpson, G., Blanchet, F., Kindt, R., Legendre, P., Minchin, P., O'Hara, R., Solymos, P., Stevens, M., Szoecs, E., Wagner, H., Barbour, M., Bedward, M., Bolker, B., Borcard, D., Carvalho, G., Chirico, M., De Caceres, M., Durand, S., Evangelista, H., FitzJohn, R., Friendly, M., Furneaux, B., Hannigan, G., Hill, M., Lahti, L., McGlinn, D., Ouellette, M., Ribeiro Cunha, E., Smith, T., Stier, A., Ter Braak, C., Weedon, J., 2022. Vegan: Community Ecology Package.

O'Leary, M.A., Bloch, J.I., Flynn, J.J., Gaudin, T.J., Giallombardo, A., Giannini, N.P., Goldberg, S.L., Kraatz, B.P., Luo, Z.-X., Meng, J., Ni, X., Novacek, M.J., Perini, F.A., Randall, Z.S., Rougier, G.W., Sargis, E.J., Silcox, M.T., Simmons, N.B., Spaulding, M., Velazco, P.M., Weksler, M., Wible, J.R., Cirranello, A.L., 2013. The placental mammal ancestor and the post–K-Pg radiation of placentals. Science 339, 662–667. https://doi.org/10.1126/science.1229237.

Olivero, E.B., 2012. Sedimentary cycles, ammonite diversity and palaeoenvironmental changes in the Upper cretaceous Marambio Group, Antarctica. Cretac. Res. 34, 348–366. https://doi.org/10.1016/j.cretres.2011.11.015.

Olivero, E.B., Ponce, J.J., Marsicano, C.A., Martinioni, D.R., 2007. Depositional Settings of the Basal López de Bertodano Formation, Maastrichtian. Antarctica. Rev. Asoc, Geológica Argent, p. 62.

Olivero, E.B., Ponce, J.J., Martinioni, D.R., 2008. Sedimentology and architecture of sharp-based tidal sandstones in the upper Marambio Group, Maastrichtian of Antarctica. Sediment. Geol. 210, 11–26. https://doi.org/10.1016/j.sedgeo.2008.07.003.

Olivero, E.B., Bedoya Agudelo, E.L., Kirschvink, J.L., Rodríguez, M., 2017. Discovery of fossiliferous breccias at the K-Pg boundary and Upper López de Bertodano Formation, Antarctica: Paleoeenvironmental interpretation. In: Visiones Sobre Ciencia Antártica. Presented at the IX Congreso Latinoamericano de Ciencia Antártica, Publicación del Instituo Antártico Chileno, Punta Arenas, Chile.

Petersen, S.V., Dutton, A., Lohmann, K.C., 2016. End-cretaceous extinction in Antarctica linked to both Deccan volcanism and meteorite impact via climate change. Nat. Commun. 7, 12079. https://doi.org/10.1038/ncomms12079.

Pielou, E.C., 1984. The Interpretation of Ecological Data: A Primer on Classification and Ordination. John Wiley & Sons.

Pimm, S.L., 1984. The complexity and stability of ecosystems. Nature 307, 321–326. https://doi.org/10.1038/307321a0.

Pirrie, D., Whitham, A.G., Ineson, J.R., 1991. The Role of Tectonics and Eustasy in the Evolution of a Marginal Basin: Cretaceous—Larsen Basin, Antarctica. Sediment. Tecton. Eustasy Sea-Level Chang. Act. Margins. https://doi.org/10.1002/9781444303896.ch17.

Pitta, E., Giokas, S., Sfenthourakis, S., 2012. Significant pairwise co-occurrence patterns are not the rule in the majority of biotic communities. Diversity 4, 179–193. https://doi.org/10.3390/d4020179.

Podani, J., Schmera, D., 2011. A new conceptual and methodological framework for exploring and explaining pattern in presence – absence data. Oikos 120, 1625–1638. https://doi.org/10.1111/j.1600-0706.2011.19451.x.

Presley, S.J., Higgins, C.L., Willig, M.R., 2010. A comprehensive framework for the evaluation of metacommunity structure. Oikos 119, 908–917. https://doi.org/10.1111/j.1600-0706.2010.18544.x.

Proulx, S., Promislow, D., Phillips, P., 2005. Network thinking in ecology and evolution. Trends Ecol. Evol. 20, 345–353. https://doi.org/10.1016/j.tree.2005.04.004.

R Core Team, 2022. R: A Language and Environment for Statistical Computing.

Reguero, M.A., 2019. Antarctic Paleontological Heritage: Late Cretaceous– Paleogene Vertebrates From Seymour (Marambio) Island, Antarctic Peninsula 30.

Rinaldi, C.A., 1992. Geologia de la Isla James Ross. Instituto Antártico Argentino.

Rinaldi, C., Massabie, A., Morelli, J., Rosenman, H.L., Del Valle, R., 1978. Geologia de la Isla Vicecomodoro Marambio. Contrib. Inst, Antártico Argent, p. 217.

Schoene, B., Eddy, M.P., Samperton, K.M., Keller, C.B., Keller, G., Adatte, T., Khadri, S.F. R., 2019. U-Pb constraints on pulsed eruption of the Deccan Traps across the end-cretaceous mass extinction. Science 363, 862–866. https://doi.org/10.1126/science.aau2422.

Solé, R.V., Montoya, J.M., Erwin, D.H., 2002. Recovery after mass extinction: evolutionary assembly in large–scale biosphere dynamics. Philos. Trans. R. Soc. Lond. Ser. B Biol. Sci. 357, 697–707. https://doi.org/10.1098/rstb.2001.0987.

Solé, R.V., Saldaña, J., Montoya, J.M., Erwin, D.H., 2010. Simple model of recovery dynamics after mass extinction. J. Theor. Biol. 267, 193–200. https://doi.org/10.1016/j.jtbi.2010.08.015.

Sprain, C.J., Renne, P.R., Vanderkluysen, L., Pande, K., Self, S., Mittal, T., 2019. The eruptive tempo of Deccan volcanism in relation to the Cretaceous-Paleogene boundary. Science 363, 866–870. https://doi.org/10.1126/science.aav1446.

Springer, M.S., 1990. The effect of random range truncations on patterns of evolution in the fossil record. Paleobiology 16, 512–520. https://doi.org/10.1017/s0094837300010228.

Steuber, T., Mitchell, S.F., Buhl, D., Gunter, G., Kasper, H.U., 2002. Catastrophic extinction of Caribbean rudist bivalves at the Cretaceous-Tertiary boundary. Geology 30, 999. https://doi.org/10.1130/0091-7613(2002)030%253C0999:CEOCRB%253E2.0.CO;2.

Stilwell, J.D., Zinsmeister, W.J., Oleinik, A., 2004. Early paleocene mollusks of antarctica: systematics, paleoecology, and paleobiogeographic significance. Bull. Am. Paleontol. 367.

Thayer, C.W., 1979. Biological bulldozers and the evolution of marine benthic communities. Science 203, 458–461. https://doi.org/10.1126/science.203.4379.458.

Tobin, T.S., 2017. Recognition of a likely two phased extinction at the K-Pg boundary in Antarctica. Sci. Rep. 7, 16317. https://doi.org/10.1038/s41598-017-16515-x.

Tobin, T.S., Ward, P.D., Steig, E.J., Olivero, E.B., Hilburn, I.A., Mitchell, R.N., Diamond, M.R., Raub, T.D., Kirschvink, J.L., 2012. Extinction patterns, δ18 O trends, and magnetostratigraphy from a southern high-latitude Cretaceous–Paleogene section: Links with Deccan volcanism. Palaeogeogr. Palaeoclimatol. Palaeoecol. 350–352, 180–188. https://doi.org/10.1016/j.palaeo.2012.06.029.

Veech, J.A., 2013. A probabilistic model for analysing species co-occurrence: probabilistic model. Glob. Ecol. Biogeogr. 22, 252–260. https://doi.org/10.1111/j.1466-8238.2012.00789.x.

Whittle, R.J., Hunter, A.W., Cantrill, D.J., McNamara, K.J., 2018. Globally discordant isocrinida (crinoidea) migration confirms asynchronous marine mesozoic revolution. Commun. Biol. 1, 46. https://doi.org/10.1038/s42003-018-0048-0.

Whittle, R.J., Witts, J.D., Bowman, V.C., Crame, J.A., Francis, J.E., Ineson, J., 2019. Nature and timing of biotic recovery in Antarctic benthic marine ecosystems following the Cretaceous–Palaeogene mass extinction. Palaeontology 62, 919–934. https://doi.org/10.1111/pala.12434.

Witts, J.D., Bowman, V.C., Wignall, P.B., Alistair Crame, J., Francis, J.E., Newton, R.J., 2015. Evolution and extinction of Maastrichtian (late cretaceous) cephalopods from the López de Bertodano Formation, Seymour Island, Antarctica. Palaeogeogr. Palaeoclimatol. Palaeoecol. 418, 193–212. https://doi.org/10.1016/j.palaeo.2014.11.002.

Witts, J.D., Whittle, R.J., Wignall, P.B., Crame, J.A., Francis, J.E., Newton, R.J., Bowman, V.C., 2016. Macrofossil evidence for a rapid and severe Cretaceous–Paleogene mass extinction in Antarctica. Nat. Commun. 7, 11738. https://doi.org/10.1038/ncomms11738.

Wright, D.H., Patterson, B.D., Mikkelson, G.M., Cutler, A., Atmar, W., 1998. A comparative analysis of nested subset patterns of species composition. Oecologia 113, 1–20.

Zinsmeister, W.J., 1982. First U.S. Expedition to the James Ross Island Area, Antarctic Peninsula. Antarct. J. U. S, 17, pp. 63–64.

Zinsmeister, W.J., 1985. 1985 Seymour Island expedition. Antarct. J. US 20, 41–42.

Zinsmeister, W.J., 1998. Discovery of fish mortality horizon at the K-T Boundary on Seymour Island: re-evaluation of events at the end of the cretaceous. J. Paleolimnol. 72, 556–571. https://doi.org/10.1017/S0022336000024331.

Zinsmeister, W.J., 2001. Late maastrichtian short-term biotic events on Seymour Island, Antarctic Peninsula. J. Geol. 109, 213–229. https://doi.org/10.1086/319239.

Zinsmeister, W.J., Feldmann, R.M., Woodburne, M.O., Elliot, D.H., 1989. Latest cretaceous/Earliest Tertiary transition on Seymour Island, Antarctica. J. Paleontol. 63, 731–738.